

# GAUGE FIELDS, STRINGS, SOLITONS, ANOMALIES, AND THE SPEED OF LIFE

Antti J. Niemi<sup>1,2,3,\*</sup>

<sup>1</sup> *Laboratoire de Mathématiques et Physique Théorique CNRS UMR 6083,  
Fédération Denis Poisson, Université de Tours,  
Parc de Grandmont, F37200, Tours, France*

<sup>2</sup> *Department of Physics and Astronomy, Uppsala University,  
P.O. Box 803, S-75108, Uppsala, Sweden*

<sup>3</sup> *Department of Physics, Beijing Institute of Technology,  
Haidian District, Beijing 100081, P. R. China*

## Abstract

It's been said that *mathematics is biology's next microscope, only better; biology is mathematics' next physics, only better* [1]. Here we aim for something even better. We try to combine mathematical physics and biology into a picoscope of life. For this we merge techniques which have been introduced and developed in modern mathematical physics, largely by Ludvig Faddeev to describe objects such as solitons and Higgs and to explain phenomena such as anomalies in gauge fields. We propose a synthesis that can help to resolve the protein folding problem, one of the most important conundrums in all of science. We apply the concept of gauge invariance to scrutinize the extrinsic geometry of strings in three dimensional space. We evoke general principles of symmetry in combination with Wilsonian universality and derive an essentially unique Landau-Ginzburg energy that describes the dynamics of a generic string-like configuration in the far infrared. We observe that the energy supports topological solitons, that pertain to an anomaly in the manner how a string is framed around its inflection points. We explain how the solitons operate as modular building blocks from which folded proteins are composed. We describe crystallographic protein structures by multi-solitons with experimental precision, and investigate the non-equilibrium dynamics of proteins under varying temperature. We simulate the folding process of a protein at *in vivo* speed and with close to pico-scale accuracy using a standard laptop computer: With pico-biology as mathematical physics' next pursuit, things can only get better.

This article is dedicated to Ludvig Faddeev on the occasion of his 80<sup>th</sup> birthday.

---

\*Electronic address: Antti.Niemi@physics.uu.se

## I. INTRODUCTION

Ludvig Faddeev is the first to draw my attention to the following sentence in the introduction of Dirac's stunning 1931 article [2],

*"There are at present fundamental problems in theoretical physics awaiting solution, e.g. the relativistic formulation of quantum mechanics and the nature of atomic nuclei (to be followed by more difficult ones such as the problem of life)."*

This epitomizes what could be proclaimed as *the three Dirac problems in theoretical physics*. The first Dirac problem was *de facto* solved at the time of writing. Dirac introduced his equation in 1928. Maybe he already had quantum gravity in his mind; it has been stated in exalted circles that this is a problem settled by string theory. A resolution to the second Dirac problem, *the nature of atomic nuclei*, took almost half-a-century of collective efforts to develop. We now trust that LHC experiments at CERN demonstrate how all four known fundamental interactions are governed by the Standard Model of Weinberg-Salam and quantum chromodynamics, plus Einstein's gravity. However, there remain important conundrums awaiting solution, including that of quark (color) confinement.

The third Dirac problem, *life*, endures. Its inclusion demonstrates Dirac's very high level of ambition, and trust on the mastery of theoretical physics. How could Dirac envisage that the notion of life could be defined as a theoretical physics problem? Did he presume that eventually life can be described with a conceptual clarity that compares with quantum mechanics?

Today we are reaching a point where a precise definition of *the problem of life* could be attempted: We understand that proteins are the workhorses of all living cells. They participate in all the metabolic activities that constitute life, as we know it. We have learned that the biological function of a protein relates intimately to its shape. Thus one might argue that the *protein folding problem* is the way to address the *problem of life* à la Dirac. The quest is to describe the folding and dynamics of proteins with the eloquence of equations in Dirac's 1931 article.

## II. ABELIAN HIGGS MODEL

The Abelian Higgs Model (AHM) and its generalizations [3] comprise the paradigm theoretical framework for describing physical scenarios, from cosmic strings to vortices in superconductors. The Weinberg-Salam model of electroweak interactions is a non-Abelian epitome of AHM, and so are the various editions of Grand Unified Theory that aim to unify all sub-atomic forces. In the sequel we shall argue that a discretized version of AHM might even describe the dynamics and folding of proteins, with sub-atomic precision and at the *speed of life*.

The elemental AHM comprises a single complex scalar field  $\phi$  and a vector field  $A_i$ . These fields are subjected to the U(1) gauge transformation

$$\begin{aligned}\phi &\rightarrow e^{ie\vartheta}\phi \\ A_i &\rightarrow A_i + \partial_i\vartheta\end{aligned}\tag{1}$$

where  $\vartheta$  is a function, and  $e$  is a parameter. We may also introduce another set of variables  $(J_i, \rho, \theta)$  that relate to  $(A_i, \phi)$  by the following change of variables,

$$\begin{aligned}\phi &= \rho \cdot e^{i\theta} \\ A_i &\rightarrow J_i = \frac{i}{2e|\phi|^2} [\phi^*(\partial_i - ieA_i)\phi - c.c.] \end{aligned} \quad (2)$$

These new variables can be introduced whenever  $\rho \neq 0$ . The  $\rho$  and  $J_i$  are both gauge invariant, they remain intact under the transformation (1). But

$$\theta \rightarrow \theta + \vartheta$$

The standard AHM Hamiltonian is

$$\mathcal{H} = \frac{1}{4} F_{ij}^2 + |(\partial_i - ieA_i)\phi|^2 + \lambda (|\phi|^2 - v^2)^2 \quad (3)$$

where

$$F_{ij} = \partial_i A_j - \partial_j A_i$$

This is the *unique* Landau-Ginsburg Hamiltonian of the AHM multiplet, within the framework of Wilsonian universality [4, 5] and invariance under the U(1) gauge transformation (1), except that in odd dimensions  $D$  a Chern-Simons term ( $ChS$ ) could be added to break parity

$$\begin{aligned} D=1 : \quad ChS &\sim A \\ D=3 : \quad ChS &\sim AdA \\ D=5 : \quad ChS &\sim AdAdA \\ &etc. \end{aligned} \quad (4)$$

The gauge invariance of (3) becomes manifest when we write it in terms of the new variables (2),

$$\mathcal{H} = \frac{1}{4} \left( J_{ij} + \frac{2\pi}{e} \sigma_{ij} \right)^2 + (\partial_i \rho)^2 + \rho^2 J_i^2 + \lambda (\rho^2 - \eta^2)^2 + ChS \quad (5)$$

Here

$$J_{ij} = \partial_i J_j - \partial_j J_i$$

and

$$\sigma_{ij} = \frac{1}{2\pi} [\partial_i, \partial_j] \theta \quad (6)$$

The  $\sigma_{ij}$  is a string current, its support coincides with the world-sheet of the cores of Abrikosov vortices. When (5) describes a vortex, (6) subtracts a singular string contribution that appears in  $J_{ij}$ . An irregular contribution then appears in the third term in the *r.h.s.* of (5) but becomes removed by the density  $\rho$  which vanishes on the world-sheet of the vortex core. Note that except along a vortex line the Hamiltonian (5) involves only variables that are manifestly U(1) gauge invariant. In particular, unlike in the case of (3), in (5) the local gauge invariance is entirely removed. *Not* by fixing a gauge but by changing the variables [6].

### III. STRINGS AND THE FRENET EQUATION

Proteins are string-like objects. Thus, to describe their physical properties we need to develop the formalism of strings. We start with the continuum (differentiable) case.

The geometry of a class  $\mathcal{C}^3$  differentiable string  $\mathbf{x}(z)$  in  $\mathbb{R}^3$  is governed by the Frenet equation [7]. Here  $z \in [0, L]$  and  $L$  is the length of the string in  $\mathbb{R}^3$  that is computed by

$$L = \int_0^L dz \|\mathbf{x}_z\| = \int_0^L dz \sqrt{\mathbf{x}_z \cdot \mathbf{x}_z} \equiv \int_0^L dz \sqrt{g}. \quad (7)$$

We recognize in (7) the (static) Nambu-Goto action; the parameter  $z \in [0, L]$  is generic. We may always reparametrize the string and express it in terms of the arc-length  $s \in [0, L]$  in the ambient  $\mathbb{R}^3$ . This is achieved by the change of variables

$$s(z) = \int_0^z \|\mathbf{x}_z(z')\| dz'$$

In the following we use the arc-length parametrization. We shall also consider a single open string and we assume that the string does not self-cross *i.e.* it is self-avoiding.

At a generic point along the string, we introduce the unit length tangent vector

$$\mathbf{t} = \frac{d\mathbf{x}(s)}{ds} \equiv \mathbf{x}_s \quad (8)$$

the unit length bi-normal vector

$$\mathbf{b} = \frac{\mathbf{x}_s \times \mathbf{x}_{ss}}{\|\mathbf{x}_s \times \mathbf{x}_{ss}\|} \quad (9)$$

and the unit length normal vector,

$$\mathbf{n} = \mathbf{b} \times \mathbf{t} \quad (10)$$

These three vectors  $(\mathbf{n}, \mathbf{b}, \mathbf{t})$  form the right-handed orthonormal Frenet frame. This framing can be introduced at each point where

$$\mathbf{x}_s \times \mathbf{x}_{ss} \neq 0 \quad (11)$$

We proceed, momentarily, by assuming this to be the case. The Frenet equation [7] transects the frames along the string,

$$\frac{d}{ds} \begin{pmatrix} \mathbf{n} \\ \mathbf{b} \\ \mathbf{t} \end{pmatrix} = \begin{pmatrix} 0 & \tau & -\kappa \\ -\tau & 0 & 0 \\ \kappa & 0 & 0 \end{pmatrix} \begin{pmatrix} \mathbf{n} \\ \mathbf{b} \\ \mathbf{t} \end{pmatrix} \quad (12)$$

where

$$\kappa(s) = \frac{\|\mathbf{x}_s \times \mathbf{x}_{ss}\|}{\|\mathbf{x}_s\|^3} \quad (13)$$

is the curvature of the string on the osculating plane that is spanned by  $\mathbf{t}$  and  $\mathbf{n}$ , and

$$\tau(s) = \frac{(\mathbf{x}_s \times \mathbf{x}_{ss}) \cdot \mathbf{x}_{sss}}{\|\mathbf{x}_s \times \mathbf{x}_{ss}\|^2} \quad (14)$$

is the torsion that measures how the string deviates from its osculating plane. Both  $\kappa(s)$  and  $\tau(s)$  are preordained solely by the extrinsic geometry *i.e.* shape of the string. According to (12), the curvature and torsion also determine the string: If the two are known we construct  $\mathbf{t}(s)$  by solving the Frenet equation and then solve for the string by integrating (8). The solution is unique up to rigid translations and rotations of the string.

We note that the curvature (13) and the torsion (14) are scalars under reparametrizations. Under an infinitesimal local diffeomorphism along the string, obtained by deforming  $s$  according to

$$s \rightarrow s + \epsilon(s) \quad (15)$$

where  $\epsilon(s)$  is an arbitrary infinitesimally small function such that

$$\epsilon(0) = \epsilon(L) = 0 = \epsilon_s(0) = \epsilon_s(L)$$

we have

$$\begin{aligned} \delta\kappa(s) &= -\epsilon(s) \kappa_s \\ \delta\tau(s) &= -\epsilon(s) \tau_s \end{aligned} \quad (16)$$

The Lie algebra of diffeomorphisms (15) is the classical Virasoro (Witt) algebra.

#### IV. ABELIAN GAUGE FIELDS

From the extrinsic string geometry we can construct an exemplar Abelian Higgs Multiplet [8–10]. For this we observe that (8) does not engage the normal and bi-normal vectors. Thus a SO(2) rotation around  $\mathbf{t}(s)$  that sends the zweibein  $(\mathbf{n}, \mathbf{b})$  into another zweibein  $(\mathbf{e}_1, \mathbf{e}_2)$  as shown in figure 1, leaves the string intact.

The generic zweibein is obtained from the Frenet zweibein as follows,

$$\begin{pmatrix} \mathbf{n} \\ \mathbf{b} \end{pmatrix} \rightarrow \begin{pmatrix} \mathbf{e}_1 \\ \mathbf{e}_2 \end{pmatrix} = \begin{pmatrix} \cos \eta(s) & \sin \eta(s) \\ -\sin \eta(s) & \cos \eta(s) \end{pmatrix} \begin{pmatrix} \mathbf{n} \\ \mathbf{b} \end{pmatrix}. \quad (17)$$

For the Frenet equation this yields

$$\frac{d}{ds} \begin{pmatrix} \mathbf{e}_1 \\ \mathbf{e}_2 \\ \mathbf{t} \end{pmatrix} = \begin{pmatrix} 0 & (\tau + \eta_s) & -\kappa \cos \eta \\ -(\tau + \eta_s) & 0 & \kappa \sin \eta \\ \kappa \cos \eta & -\kappa \sin \eta & 0 \end{pmatrix} \begin{pmatrix} \mathbf{e}_1 \\ \mathbf{e}_2 \\ \mathbf{t} \end{pmatrix}. \quad (18)$$

Remarkably, by interpreting  $\kappa(s)$  as the modulus of a complex quantity

$$\kappa \xrightarrow{\eta} \kappa e^{-i\eta} \quad (19)$$

we may consider the transition of  $(\kappa, \tau)$  in (17) as a one-dimensional example of the U(1) gauge transformation (1), with curvature identified as the Higgs field and torsion as the gauge field,

$$\begin{aligned} \kappa \sim \phi &\rightarrow \kappa e^{-i\eta} \equiv \phi e^{-i\eta} \\ \tau \sim A_i &\rightarrow \tau + \eta_s \equiv A_i + \eta_s \end{aligned} \quad (20)$$

We remark that the choice

$$\eta(s) = - \int_0^s \tau(\tilde{s}) d\tilde{s} \quad (21)$$

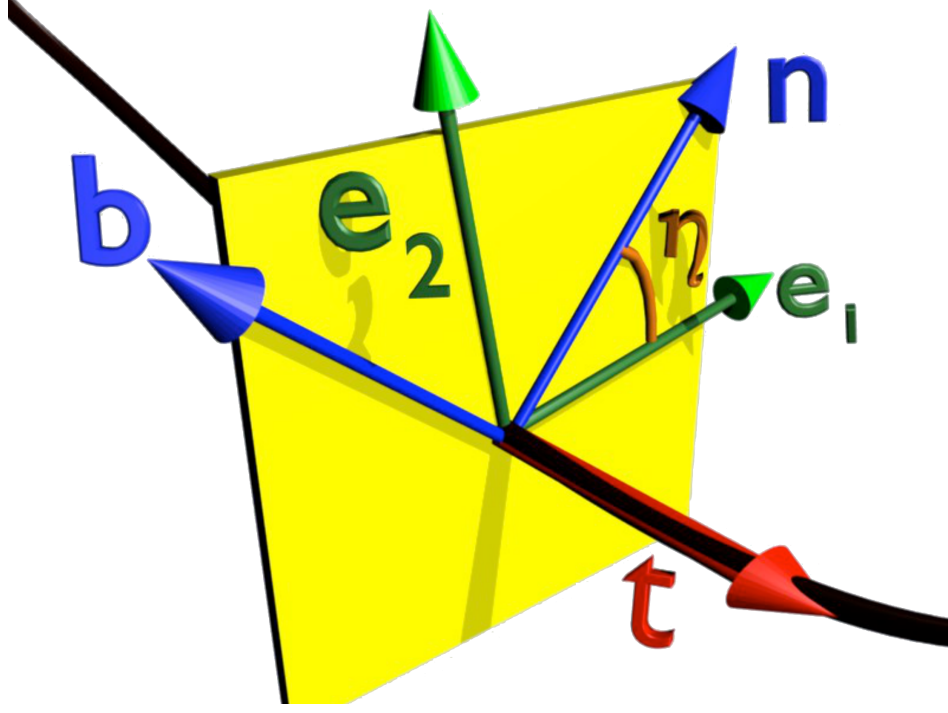


FIG. 1: Rotation between the Frenet frames and generic frames on the normal plane of the string.

brings about the *unitary* gauge, that corresponds to the parallel transport framing [11]. Unlike the Frenet framing that can not be defined at points (or segments) where (11) vanishes, the parallel transport framing can still be defined in a continuous manner [12]. But there is an anomaly lurking, that we soon reveal.

## V. SPINOR FRENET EQUATION

Occasionally, it is profitable to recognize that the Frenet equation admits a spinor representation [10]. For this we introduce a two-component complex spinor

$$\psi = \begin{pmatrix} z_1 \\ z_2 \end{pmatrix} \quad (22)$$

We also introduce the conjugate spinor  $\bar{\psi}$ ; the two are related by the charge conjugation operation  $\mathcal{C}$ ,

$$\bar{\psi} = \mathcal{C}\psi = -i\sigma^2\psi^* = \begin{pmatrix} -z_2^* \\ z_1^* \end{pmatrix} \quad (23)$$

Note that

$$\mathcal{C}^2 = -\mathbb{I}$$

We impose the normalization condition

$$\psi^\dagger\psi \equiv \langle \psi, \psi \rangle = 1 = \langle \bar{\psi}, \bar{\psi} \rangle = \bar{\psi}^\dagger\bar{\psi} \quad (24)$$

$$\langle \psi, \bar{\psi} \rangle = 0$$

We define the spin polarization vector  $\mathbf{t}$  so that

$$\mathbf{t} \cdot \hat{\sigma} \psi = \psi \quad \Leftrightarrow \quad \mathbf{t} \cdot \hat{\sigma} \bar{\psi} = -\bar{\psi} \quad (25)$$

We get

$$\mathbf{t} = \psi^\dagger \hat{\sigma} \psi = \langle \psi, \hat{\sigma} \psi \rangle$$

We also define the following complex vector,

$$\mathbf{e}_+ = \mathbf{e}_1 + i\mathbf{e}_2 = \langle \bar{\psi}, \hat{\sigma} \psi \rangle \equiv \bar{\psi}^\dagger \hat{\sigma} \psi$$

where  $\mathbf{e}_1$  and  $\mathbf{e}_2$  are real. We can check that

$$\mathbf{e}_i \cdot \mathbf{e}_j = \delta_{ij} \quad \& \quad \mathbf{e}_i \cdot \mathbf{t} = 0$$

and we conclude that  $(\mathbf{e}_1, \mathbf{e}_2, \mathbf{t})$  is a right-handed orthonormal system. It can be identified with a Frenet framing of a string defined by  $\mathbf{t}(s)$  as the tangent vector, possibly modulo a global  $\text{SO}(2)$  frame rotation.

Consider the following local  $\text{U}(1)$  rotation:

$$\psi \rightarrow e^{in} \psi \quad \& \quad \bar{\psi} \rightarrow e^{-in} \bar{\psi} \quad (26)$$

Then,

$$\langle \psi, \partial_s \psi \rangle = \psi^\dagger \partial_s \psi \rightarrow \langle \psi, \partial_s \psi \rangle + i \partial_s n$$

This suggest we introduce the putative *torsion*

$$\tau \sim -i \langle \psi, \partial_s \psi \rangle \quad (27)$$

Furthermore, since

$$\langle \bar{\psi}, \partial_s \psi \rangle = \bar{\psi}^\dagger \partial_s \psi \rightarrow e^{2in} \langle \bar{\psi}, \partial_s \psi \rangle$$

we identify

$$\kappa \sim \langle \bar{\psi}, \partial_s \psi \rangle \sim \kappa \quad (28)$$

as the putative (complex) *curvature*. Thus, we have the *spinor Frenet equation*:

$$\partial_s \psi = i\tau \psi + \kappa \bar{\psi} \quad (29)$$

If curvature and torsion in (29) are known, we can solve for  $\psi$  and compute

$$\mathbf{t} = \langle \psi, \hat{\sigma} \psi \rangle$$

The string in the arc-length parametrization is then determined as before, from

$$\frac{d\mathbf{x}}{ds} = \mathbf{t}$$

## VI. NON-ABELIAN GAUGE FIELDS

The geometric interpretation of curvature and torsion in terms of the AHM multiplet extends to a non-Abelian framework. This brings about a relation between extrinsic string geometry and the structure of non-Abelian gauge theories, in a decomposed format of the latter [13–16]. These relations are valuable for a wider perspective, beyond the immediate scope of the present article: We start by introducing the three matrices

$$T_1 = \begin{pmatrix} 0 & 0 & 0 \\ 0 & 0 & -1 \\ 0 & 1 & 0 \end{pmatrix}, \quad T_2 = \begin{pmatrix} 0 & 0 & 1 \\ 0 & 0 & 0 \\ -1 & 0 & 0 \end{pmatrix}, \quad T_3 = \begin{pmatrix} 0 & -1 & 0 \\ 1 & 0 & 0 \\ 0 & 0 & 0 \end{pmatrix} \quad (30)$$

that determine the canonical adjoint representation of  $\underline{\text{so}}(3)$  Lie algebra,

$$[T_a, T_b] = \epsilon_{abc} T_c.$$

The action of the  $\text{SO}(2) \sim \text{U}(1)$  frame rotation on  $\kappa$  and  $\tau$  may be realized as follows,

$$\kappa T_2 \rightarrow e^{-\eta T_3} (\kappa T_2) e^{\eta T_3} = \kappa (\cos \eta T^2 - \sin \eta T^1), \quad (31)$$

$$\tau T_3 \rightarrow (\tau + \eta') T_3. \quad (32)$$

This proposes that we combine the (general frame) curvature and torsion into a non-Abelian  $\text{SO}(3)$  gauge field

$$A^a T^a = A^1 T^1 + A^2 T^2 + A^3 T^3 = \kappa \sin \eta T^1 + \kappa \cos \eta T^2 + \tau_\eta T^3 \quad (33)$$

The  $\text{SO}(3)$  gauge transformation

$$A^a T^a \rightarrow g^{-1} (A^a T^a + i \partial_s) g$$

corresponds to a general frame rotation while (31), (32) determine the subset of  $\text{SO}(2)$  gauge transformations in the Cartan direction

$$g = e^{\eta T^3}$$

The spinor Frenet equation can be interpreted as follows: We combine the two spinors (22), (23) into a four component Majorana spinor

$$\Psi = \frac{1}{\sqrt{2}} \begin{pmatrix} \psi \\ \bar{\psi} \end{pmatrix}$$

Using (27), (28) we recover the connection (33), now in the  $\text{SU}(2)$  basis,

$$\begin{aligned} A^a T^a &\sim \mathcal{A}_{\alpha\beta} = \Psi_\alpha^\dagger \partial_s \Psi_\beta = \begin{pmatrix} \tau & -i\kappa \\ i\kappa^* & -\tau \end{pmatrix} = \mathcal{A} \cdot \hat{\sigma} \\ &= \tau \sigma^3 + \kappa_1 \sigma^1 + \kappa_2 \sigma^2 \equiv \tau \sigma^3 + \kappa \sigma^+ + \kappa^* \sigma^- \end{aligned} \quad (34)$$

$$\kappa_1 = \Re[\kappa] \quad \& \quad \kappa_2 = \Im[\kappa]$$



Then we have from (29) for the Frenet equation

$$(i\partial_s + \mathcal{A} \cdot \hat{\sigma}) \Psi = 0 \quad (35)$$

which remains covariant under the SU(2) gauge transformation

$$\Psi \rightarrow g\Psi \equiv \Psi_g \quad \Rightarrow \quad \mathcal{A} \rightarrow g(\mathcal{A} + i\partial_s)g^{-1} \equiv \mathcal{A}_g$$

corresponding to a general  $SO(3) \simeq SU(2)$  rotation of frames, along the string. Of particular interest is the gauge transformation defined by  $g \in SU(2)$  so that

$$\begin{aligned} g\sigma^3g^{-1} &= \mathbf{t} \cdot \hat{\sigma} \equiv \hat{\mathbf{t}} \\ g(\sigma^1 + i\sigma^2)g^{-1} &= (\mathbf{n} + i\mathbf{b}) \cdot \hat{\sigma} \equiv \mathbf{e}_+ \cdot \hat{\sigma} = \hat{\mathbf{e}}_+ \end{aligned}$$

This identifies the Frenet framing and sends (34) into

$$\mathcal{A} \cdot \hat{\sigma} \rightarrow (\tau \hat{\mathbf{t}} + \kappa \hat{\mathbf{e}}_+ + \kappa^* \hat{\mathbf{e}}_-) + \mathbf{a} \hat{\mathbf{t}} + \frac{1}{2i} [\partial_s \hat{\mathbf{t}}, \hat{\mathbf{t}}] \quad (36)$$

$$\mathbf{a} = 2i \langle \mathbf{e}^+, \partial_s \mathbf{e}^- \rangle$$

The SU(2) connection (36) has the functional form of the decomposed connection introduced in [13], including the "monopole" contribution. In particular, the  $U(1) \in SU(2)$  gauge rotation around the Cartan direction  $\hat{\mathbf{t}}$  [13]

$$g = \exp\{i\frac{\eta}{2}\hat{\mathbf{t}}\}$$

sends

$$\begin{aligned} \kappa &\rightarrow e^{i\eta}\kappa \\ \tau &\rightarrow \tau + \partial_s \eta \\ \mathbf{a} &\rightarrow \mathbf{a} + \partial_s \eta \end{aligned}$$

This is the same as (17), (18). The present construction divulges that there is an intrinsic string design hiding in non-Abelian gauge theories.

## VII. ENERGY OF STRING

To describe string dynamics, and eventually that of proteins, we desire an energy function in terms of the curvature and torsion. For this we remind that the Landau-Ginzburg energy (3) of the elemental AHM is *unique* in the Wilsonian sense of universality. It emerges from general arguments and symmetry principles alone. We also remind that the shape of a string does not depend on the way how we frame it. Accordingly, the energy of a string can only engage manifestly frame independent combinations of the curvature and torsion (20). Since (3) is the universal  $SO(2) \sim U(1)$  invariant energy function that involves a complex Higgs field  $\phi \sim \kappa$  and a gauge field  $A \sim \tau$ , it must serve as the Hamiltonian that describes strings and their dynamics in the far infrared. Thus, we introduce

$$H = \int_0^L ds \left\{ |(\partial_s + ie\tau)\kappa|^2 + \lambda(|\kappa|^2 - m^2)^2 \right\} + a \int_0^L ds \tau \quad (37)$$

We have included the one dimensional version of the Chern-Simons term (4), it introduces chirality to the string; in one dimension there is no  $F_{ij}$ .

In (37), the curvature  $\kappa$  and torsion  $\tau$  are expressed in a generic, arbitrary framing of the string. The ensuing gauge invariant variables (2) coincide with the Frenet frame curvature (13) and torsion (14) that characterize the extrinsic string geometry. In terms of these *gauge invariant variables*, which we *from now on* denote by  $(\kappa, \tau)$  the Hamiltonian (37) becomes

$$H = \int_0^L ds \{ (\partial_s \kappa)^2 + e^2 \kappa^2 \tau^2 + \lambda (\kappa^2 - m^2)^2 \} + a \int_0^L ds \tau \quad (38)$$

This is our manifestly gauge invariant Landau-Ginzburg Hamiltonian of strings; see (5).

Finally, we point out a non-Abelian variant of the energy: A solution to the equation (35) minimizes the functional

$$\mathcal{S} = \int ds |(i\partial_s + \mathcal{A})\Psi|^2$$

This is an exemplar of the gauged SU(2) non-linear  $\sigma$ -model; recall that the Majorana spinor is subject to the normalization condition that derives from (24). Additional SU(2) gauge invariant functionals of  $(\Psi, \mathcal{A})$  could be introduced. This leads to gauged non-linear  $\sigma$ -models as energy functions of strings.

## VIII. INTEGRABLE HIERARCHY

There is a relation between (38), the integrable hierarchy of the nonlinear Schrödinger (NLS) equation, and the Heisenberg spin chain. For this we follow Hasimoto [17] and combine the curvature and torsion into the complex variable

$$\psi(s) = \kappa(s) e^{ie \int_0^s ds' \tau(s')} \quad (39)$$

This yields us the standard NLS Hamiltonian density [18, 19]

$$\kappa_s^2 + e^2 \kappa^2 \tau^2 + \lambda \kappa^4 = \bar{\psi}_s \psi_s + \lambda (\bar{\psi} \psi)^2 = \mathcal{H}_3 \quad (40)$$

The lower level conserved densities in the integrable NLS hierarchy are the helicity, length (*i.e.* Nambu-Goto), number operator and momentum respectively

$$\begin{aligned} \mathcal{H}_{-2} &= \tau \\ \mathcal{H}_{-1} &= L \\ \mathcal{H}_1 &= \kappa^2 \\ \mathcal{H}_2 &= \kappa^2 \tau \end{aligned} \quad (41)$$

The energy (38) is a combination of  $\mathcal{H}_{-2}$ ,  $\mathcal{H}_1$  and  $\mathcal{H}_3$ . From the perspective of the NLS hierarchy, the momentum  $\mathcal{H}_2$  could also be included. In case higher order corrections are desired, the natural candidate is the mKdV density

$$\mathcal{H}_4 = \kappa \kappa_{ss} \tau + 4 \kappa^2 \tau^3 - 4 e^2 \kappa_s^2 \tau + 3 \lambda \kappa^4 \tau$$

with appears as the next level conserved density in the NLS hierarchy.

The Heisenberg spin chain is obtained directly from  $\mathcal{H}_1$ , in terms of the Frenet equation.

$$\int_0^L ds \mathcal{H}_1 = \int_0^L ds \kappa^2 = \int_0^L ds |\mathbf{t}_s|^2$$

The combination of  $\mathcal{H}_{-1}$  and  $\mathcal{H}_1$  leads to the rigid string action [20], it also relates to Kratky-Porod model of polymer physics [21]. In [20], perturbative level Wilsonian universality is employed to argue that no additional terms should emerge in the infrared. However, a perturbative approach does not reach into the non-perturbative, the NLS Hamiltonian (40) is known to support solitons that are pivotal in the description of numerous far infrared physical phenomena.

## IX. SOLITONS

Solitons are the paradigm structural self-organizers in the physical world. They materialize in numerous scenarios [18, 19, 22, 23]: Solitons transmit data in transoceanic cables, solitons conduct electricity in organic polymers and transport chemical energy in proteins. Solitons explain the Meißner effect in superconductivity and dislocations in liquid crystals. Solitons model hadronic particles, cosmic strings and magnetic monopoles in high energy physics. In the sequel we argue that solitons might even describe life: There are about  $10^{20}$  or so solitons in your own human body. They participate in all the metabolic processes that make you kick, spark and to be alive.

The NLS equation that derives from (40) is the paradigm equation that supports solitons [18, 19, 22, 23]. Depending on the sign of  $\lambda$ , these solitons are either dark ( $\lambda > 0$ ) or bright ( $\lambda < 0$ ). Furthermore, on the real line  $\mathbb{R}$  the torsion independent contribution to (38)

$$H = \int_{-\infty}^{\infty} ds \{ \kappa_s^2 + \lambda (\kappa^2 - m^2)^2 \} \quad (42)$$

describes the double well kink *a.k.a.* the paradigm *topological* soliton: For positive  $m^2$  and when  $\kappa$  can take both positive and negative values the ensuing equation of motion

$$\kappa_{ss} = 2\lambda\kappa(\kappa^2 - m^2)$$

is solved by

$$\kappa(s) = m \tanh \left[ m\sqrt{\lambda}(s - s_0) \right] \quad (43)$$

The energy function

$$\mathcal{E} = \int ds \left\{ \kappa_s^2 + \lambda(\kappa^2 - m^2)^2 + \frac{d}{2}\kappa^2\tau^2 - b\kappa^2\tau - a\tau + \frac{c}{2}\tau^2 \right\} \quad (44)$$

is the most general linear combination of *all* the densities (40), (41). In addition we have included the Proca mass term (the last term) [9, 10]. Even though the Proca mass does not appear in the integrable NLS hierarchy, it does have a claim of gauge invariance and as such

it is often accounted for. Since (44) is quadratic in the torsion, we may eliminate  $\tau$  using the ensuing equation of motion,

$$\frac{\delta \mathcal{E}}{\delta \tau} = d\kappa^2\tau - b\kappa^2 - a + c\tau = 0 \quad (45)$$

This gives

$$\tau[\kappa] = \frac{a + b\kappa^2}{c + d\kappa^2} \quad (46)$$

Thus we obtain the following *effective* energy for the curvature,

$$\mathcal{E}_\kappa = \int ds \left\{ \frac{1}{2}\kappa_s^2 + V[\kappa] \right\} \quad (47)$$

with the equation of motion

$$\frac{\delta \mathcal{E}_\kappa}{\delta \kappa} = -\kappa_{ss} + V_\kappa = 0 \quad (48)$$

where

$$V[\kappa] = -\left(\frac{bc - ad}{d}\right) \frac{1}{c + d\kappa^2} - \left(\frac{b^2 + 8\lambda m^2}{2b}\right) \kappa^2 + \lambda \kappa^4 \quad (49)$$

This is a deformation of the potential in (42); the two share the same large- $\kappa$  asymptotics. For a suitable choice of parameters we expect that (45), (48), (49) continue to support topological solitons. But we do not know their explicit profile, in terms of elementary functions. In the sequel we construct the solitons numerically.

## X. FRAME ANOMALY

We now introduce the frame anomaly. It is the edifice of a topological soliton along the string. Thus far we have tacitly assumed (11). It ensures that the Frenet curvature (13) does not vanish. But we already pointed out that in AHM we have  $\rho = 0$  at the core of a vortex line. Moreover, the explicit profile (43) is both positive and negative, and vanishes at  $s = s_0$ . Thus the consequences of  $\kappa = 0$  for a string deserves to be investigated. For this it can be profitable to extend the Frenet curvature  $\kappa(s)$  so that it takes both positive and negative values. From (19) we conclude that the negative values of  $\kappa$  are related to the positive ones by a  $\eta = \pm\pi$  frame rotation,

$$\kappa \xrightarrow{\eta=\pm\pi} e^{\pm i\pi} \kappa = -\kappa \quad (50)$$

Hence we compensate for the extension of  $\kappa$  to negative values, by engaging a discrete  $\mathbb{Z}_2$  symmetry [33].

An (isolated) point where the curvature  $\kappa(s)$  vanishes is an inflection point. In figure 2 we show an example of an inflection point. Notice how the Frenet framing experiences a sudden change: The zweibein  $(\mathbf{n}, \mathbf{b})$  is reflected according to

$$(\mathbf{n} + i\mathbf{b}) \longrightarrow -(\mathbf{n} + i\mathbf{b}) = e^{\pm i\pi}(\mathbf{n} + i\mathbf{b}) \quad (51)$$

when it proceeds through the inflection point. At the inflection point itself the Frenet frame is not defined. Thus we can not directly determine whether there has been a jump by  $\eta = +\pi$

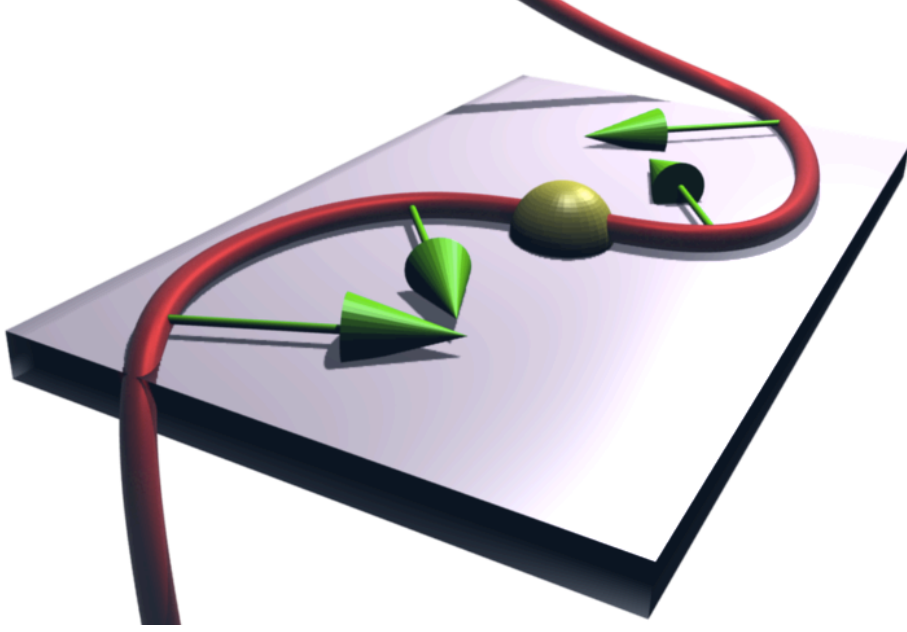


FIG. 2: A string with inflection point (ball). At each point the Frenet frame normal vector points towards the center of the osculating circle. At the inflection point there is a discontinuity in the direction of the normal vectors: The radius of the osculating circle diverges and the normal vector are reflected in the osculating plane, from one side to the other side of the string.

or by  $\eta = -\pi$  in figure 2. That is, does the frame turn left or does it turn right by  $\pi$ , at the inflection point. We have a *frame anomaly*.

To scrutinize this anomaly, we consider a string  $\mathbf{x}(s)$  that has a simple inflection point when  $s = s_0$  so that  $\kappa(s_0) = 0$  but  $\kappa_s(s_0) \neq 0$ ; for notational simplicity we here re-define the parameter  $s$  so that  $s_0 = 0$ . Since a generic string in  $\mathbb{R}^3$  has no inflection point, we may also remove it from  $\mathbf{x}(s)$  by a generic deformation. We introduce two such deformations,

$$\mathbf{x}(s) \rightarrow \mathbf{x}(s) + \delta\mathbf{x}_{1,2}(s) = \mathbf{x}_{1,2}(s) \quad (52)$$

In figure 2 these deformations would amount to a move of the string either slightly up from the plane or slightly down from the plane, to remove the inflection point; a move restricted to the plane only slides the inflection point. We assume the deformations are tiny and compactly supported so that

$$\delta\mathbf{x}_{1,2}(\pm\varepsilon_{\pm}) = 0$$

Here  $\varepsilon_{\pm} > 0$  are small and determine the parameter values where the deformations  $\mathbf{x}_{1,2}(s)$  bifurcate. We consider a closed string  $\Gamma$  that starts from  $\mathbf{x}(-\varepsilon_-)$ , follows along  $\mathbf{x}_1$  to  $\mathbf{x}(+\varepsilon_+)$  and then returns along  $\mathbf{x}_2$  back to  $\mathbf{x}(-\varepsilon_-)$ . We introduce the Frenet frame normal vectors of  $\Gamma$ , to define a second closed string  $\tilde{\Gamma}$ . It is obtained by shifting  $\Gamma$  slightly into the direction of its Frenet frame normals. Let  $\mathbf{t}$ ,  $\tilde{\mathbf{t}}$  be the ensuing tangent vectors. We compute the Gauß linking number

$$\text{Lk} = \frac{1}{4\pi} \oint_{\Gamma} \oint_{\tilde{\Gamma}} ds d\tilde{s} \frac{\mathbf{x} - \tilde{\mathbf{x}}}{|\mathbf{x} - \tilde{\mathbf{x}}|^3} \cdot (\mathbf{t} \times \tilde{\mathbf{t}})$$

When we proceed along  $\mathbf{x}_{1,2}(s)$  the respective Frenet frames become continuously rotated by  $\eta_{1,2} \approx \pm\pi$ ; in the limit where  $\delta\mathbf{x}_{1,2} \rightarrow 0$  we obtain the discontinuous jump (51). By continuity of Frenet framing in the complement of inflection points, the linking number has values  $\text{Lk} = \pm 1$  when the  $\eta_{1,2}$  change in the same direction; recall that  $\Gamma$  proceeds "backwards" along  $\mathbf{x}_2$ . But  $\text{Lk} = 0$  if the framing along  $\mathbf{x}_1(s)$  and  $\mathbf{x}_2(s)$  rotate in the opposite directions. Crucially the relative sign of  $\eta_{1,2}$  appears to depend on the way how the inflection point becomes circumvented. Thus there is a frame anomaly as  $\delta\mathbf{x}_{1,2} \rightarrow 0$ . The value of  $\text{Lk}$  depends on the way how we define  $\delta\mathbf{x}_{1,2}(s)$ .

## XI. PERESTROIKA'S

When an inflection point occurs and a frame anomaly takes place, we have a string specific bifurcation which is called *inflection point perestroika* [25–29]. It renders futile our attempts to uniquely frame the string  $\mathbf{x}(s)$  across the inflection point. But there is also another kind of perestroika that takes place at the inflection point, which we now explain:

We start with a long flat string segment, so that the torsion  $\tau(s)$  of the segment vanishes. This is synonymous for the segment to be constrained on a plane, *e.g.* as shown in figure 2. For a string on the plane a simple isolated inflection is generically present, somewhere along the string. Moreover, if we deform the string but strictly in a manner that retains it on the plane, a simple inflection point can not disappear. It only moves around, unless it escapes thru the ends of the string which we assume is not the case: For a string on the plane, a single inflection point is a topological invariant.

Consider now the string in  $\mathbb{R}^3$ . Generically, it does not have any inflection points. But if the string moves freely, an isolated simple inflection point generically appears at some isolated value of the flow parameter. Furthermore, when the ensuing inflection point perestroika takes place along the moving string, it leaves behind a trail: The *momentary* inflection point perestroika *permanently* changes the number of *flattening points* which are the points along the string where its torsion  $\tau(s)$  vanishes [28, 29].

At a simple flattening point the curvature  $\kappa(s)$  is generically non-vanishing, while the torsion  $\tau(s)$  changes its sign. Thus the inflection point perestroika can only change the number of simple flattening points by two. Apparently, it always does [28, 29].

Unlike the inflection point, a flattening point is generic in a static space string. Furthermore, unlike a simple inflection point, a single simple flattening point that occurs in a one parameter family of strings in  $\mathbb{R}^3$  is a topological invariant. It can not disappear on its own, under local deformations that do not touch the ends of the string. But a pair of flattening points may become combined into a single bi-flattening point which can dissolve. When this happens, a second string-specific bifurcation called *bi-flattening perestroika* takes place.

Apparently, inflection point perestroika and bi-flattening perestroika are the only two bifurcations where the number of flattening points can change [29]. The number of simple flattening points is a local invariant of the string. Besides the flattening number, and the self-linking number in case of a framed string, a generic smooth string does not possess any other essential local invariants [28]. The two are also mutually independent, even though they often conspire.

For example, the self-linking number of the string increases by one if the torsion is positive when the string approaches its simple inflection point, and if two simple flattening points disappear after the passage of the inflection point. Moreover, if the torsion is negative, the self-linking number decreases by one when two flattening points disappear after the

passage [28]. But when two simple flattening points dissolve in a bi-flattening perestroika, the self-linking number in general does not change.

We conclude this Section with the following *statement*: Bifurcations are the paradigm causes for restructuring transitions in any dynamical system. Perestroika's are the only known stringy versions of bifurcations. Thus perestroika's have a potentially profound influence on the physical behavior of string-like structures. Moreover, perestroika's relate to the frame anomaly which is a structural attribute of a string. This identifies perestroika's as those bifurcations, that drive string-specific phase transitions which involve structural re-organizations. In particular, perestroika's prompt topological solitons such as (43) to come and go along a string. Such processes are commonplace whenever we have an energy function of the form (44). It appears that in the case of strings that model proteins, we always do. In proteins, we find solitons and perestroika's all over the place.

## XII. DISCRETE FRENET FRAMES

Proteins are linear macromolecules with a highly complex chemical composition. Proteins are made of twenty different covalently bonded amino acid molecules (residues) that are joined together in a row, one after another. But despite the diversity of amino acids most proteins share a plenty of conformational similarities. To an extent, that their structure and dynamics can be described using a single theoretical model that concurs with a distinct universality class, in the sense of Kadanoff and Wilson [4, 5].

However, proteins are not really continuous, differentiable strings. Thus we need to extend our considerations accordingly. We start with the Frenet equations. In the "scaling limit" where the concepts of Wilsonian universality become applicable, a protein is akin a piecewise linear polygonal string. Its vertices coincide with the positions of the central C $\alpha$  carbons. See figure 3. *A priori* this reduction of the entire protein chain into a skeletal C $\alpha$  backbone is an enormous simplification. But as we shall demonstrate, it is nevertheless sufficient for describing the structure and dynamics of a protein with a sub-atomic precision. The approach we propose matches the accuracy which is obtained in ultrahigh resolution x-ray crystallography experiments.

Accordingly, we proceed to generalize the Frenet frame formalism to the case of polygonal strings that are piecewise linear. Let  $\mathbf{r}_i$  be the vertices with  $i = 1, \dots, N$ . At each vertex we introduce the unit tangent vector

$$\mathbf{t}_i = \frac{\mathbf{r}_{i+1} - \mathbf{r}_i}{|\mathbf{r}_{i+1} - \mathbf{r}_i|} \quad (53)$$

the unit binormal vector

$$\mathbf{b}_i = \frac{\mathbf{t}_{i-1} - \mathbf{t}_i}{|\mathbf{t}_{i-1} - \mathbf{t}_i|} \quad (54)$$

and the unit normal vector

$$\mathbf{n}_i = \mathbf{b}_i \times \mathbf{t}_i \quad (55)$$

The orthonormal triplet  $(\mathbf{n}_i, \mathbf{b}_i, \mathbf{t}_i)$  defines a discrete version of the Frenet frames (8)-(10) at each position  $\mathbf{r}_i$  along the string.

In lieu of the curvature and torsion, we have the bond angles and torsion angles, see figure 4. The bond angles are

$$\kappa_i \equiv \kappa_{i+1,i} = \arccos(\mathbf{t}_{i+1} \cdot \mathbf{t}_i) \quad (56)$$

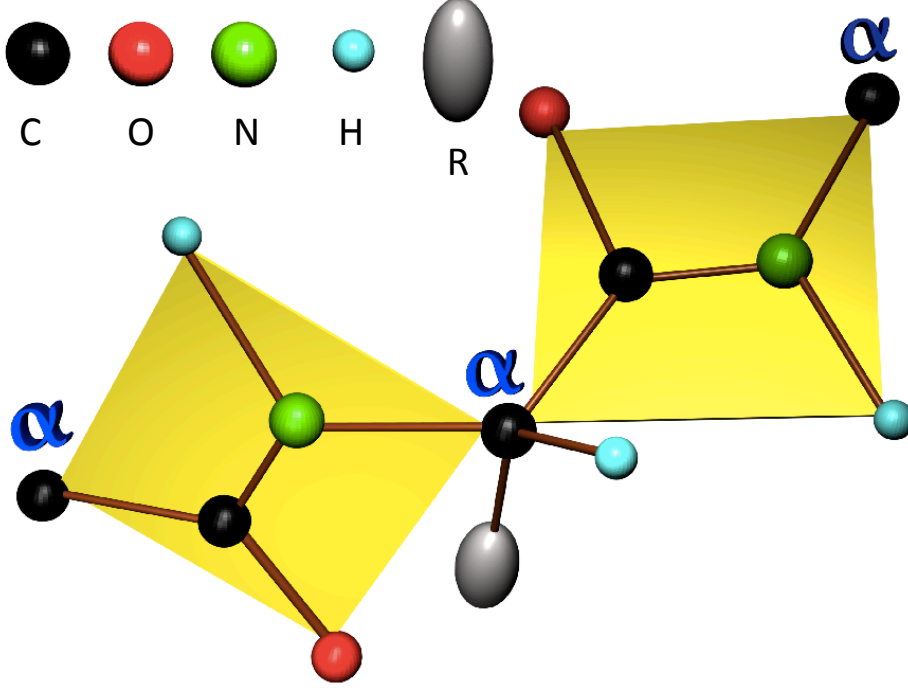


FIG. 3: All proteins are composed similarly, with an identical and *very* rigid peptide-plane structure which makes Wilsonian universality operable: The central  $C\alpha$  carbons to which the twenty different amino acids (residues  $R$ ) are attached, form the vertices that connect the peptide planes into a one dimensional discrete string. The distance between two consecutive  $C\alpha$  atoms is  $3.8 \text{ \AA}$ , except in the rare case of *cis*-proline where the distance  $2.8 \text{ \AA}$  should be used.

and the torsion angles are

$$\tau_i \equiv \tau_{i+1,i} = \text{sign}\{\mathbf{b}_{i-1} \times \mathbf{b}_i \cdot \mathbf{t}_i\} \cdot \arccos(\mathbf{b}_{i+1} \cdot \mathbf{b}_i) \quad (57)$$

When these angles are all known, we have the discrete Frenet equation

$$\begin{pmatrix} \mathbf{n}_{i+1} \\ \mathbf{b}_{i+1} \\ \mathbf{t}_{i+1} \end{pmatrix} = \begin{pmatrix} \cos \kappa \cos \tau & \cos \kappa \sin \tau & -\sin \kappa \\ -\sin \tau & \cos \tau & 0 \\ \sin \kappa \cos \tau & \sin \kappa \sin \tau & \cos \kappa \end{pmatrix}_{i+1,i} \begin{pmatrix} \mathbf{n}_i \\ \mathbf{b}_i \\ \mathbf{t}_i \end{pmatrix} \quad (58)$$

From this we obtain the frame at position  $i + 1$  from the frame at position  $i$ . Once all the frames have been constructed, the entire string is obtained from

$$\mathbf{r}_k = \sum_{i=0}^{k-1} |\mathbf{r}_{i+1} - \mathbf{r}_i| \cdot \mathbf{t}_i \quad (59)$$

Without any loss of generality we may set  $\mathbf{r}_0 = 0$ , choose  $\mathbf{t}_0$  to point into the direction of the positive  $z$ -axis, and orient  $\mathbf{t}_1$  to lie in the  $y$ - $z$  plane.

The relation (59) does not involve the vectors  $\mathbf{n}_i$  and  $\mathbf{b}_i$ . In parallel with a continuum string, our discrete string remains intact under rotations of the  $(\mathbf{n}_i, \mathbf{b}_i)$  zweibein around  $\mathbf{t}_i$ .



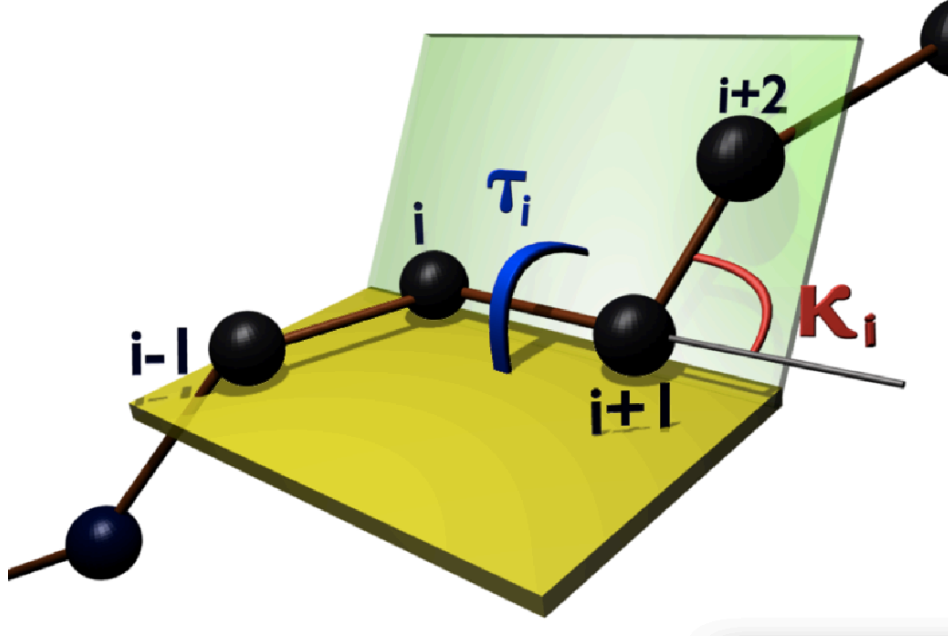


FIG. 4: Definition of bond ( $\kappa_i$ ) and torsion ( $\tau_i$ ) angles, along the discrete  $C\alpha$  string.

Such a local  $SO(2)$  rotation acts on the frames as follows

$$\begin{pmatrix} \mathbf{n} \\ \mathbf{b} \\ \mathbf{t} \end{pmatrix}_i \rightarrow e^{\Delta_i T^3} \begin{pmatrix} \mathbf{n} \\ \mathbf{b} \\ \mathbf{t} \end{pmatrix}_i = \begin{pmatrix} \cos \Delta_i & \sin \Delta_i & 0 \\ -\sin \Delta_i & \cos \Delta_i & 0 \\ 0 & 0 & 1 \end{pmatrix} \begin{pmatrix} \mathbf{n} \\ \mathbf{b} \\ \mathbf{t} \end{pmatrix}_i \quad (60)$$

Here  $\Delta_i$  is the rotation angle at vertex  $i$  and we have introduced the  $SO(3)$  generators (30). This yields the following transformation of the bond and torsion angles, *cf.* (31), (32)

$$\kappa_i T^2 \rightarrow e^{\Delta_i T^3} (\kappa_i T^2) e^{-\Delta_i T^3} \quad (61)$$

$$\tau_i \rightarrow \tau_i + \Delta_{i-1} - \Delta_i \quad (62)$$

Since the  $\mathbf{t}_i$  remain intact under (60), this transformation of  $(\kappa_i, \tau_i)$  has no effect on the discrete string geometry.

*A priori*, the fundamental range of the bond angle is  $\kappa_i \in [0, \pi]$  while for the torsion angle the range is  $\tau_i \in [-\pi, \pi)$ . Thus we identify  $(\kappa_i, \tau_i)$  as the canonical latitude and longitude angles of a two-sphere  $\mathbb{S}^2$ . In parallel with the continuum case we find it useful to extend the range of  $\kappa_i$  into negative values  $\kappa_i \in [-\pi, \pi] \bmod(2\pi)$ . As in (50) we compensate for this two-fold covering of  $\mathbb{S}^2$  by the discrete  $\mathbb{Z}_2$  symmetry

$$\begin{aligned} \kappa_k &\rightarrow -\kappa_k & \text{for all } k \geq i \\ \tau_i &\rightarrow \tau_i - \pi \end{aligned} \quad (63)$$

We note that this is a special case of (61), (62), with

$$\begin{aligned} \Delta_k &= \pi & \text{for } k \geq i+1 \\ \Delta_k &= 0 & \text{for } k < i+1 \end{aligned}$$

### XIII. DISCRETIZED ENERGY

According to (58) the bond and torsion angles are the natural variables for constructing energy functions for discrete piecewise linear strings. In analogy with the continuum case, the energy must remain invariant under the local  $SO(2)$  frame rotation (61), (62). We consider a generic energy function  $H(\kappa, \tau)$  which is  $SO(2)$  invariant. We assume  $H(\kappa, \tau)$  has an extremum with bond and torsion angle values  $\kappa_i = \kappa_{i0}$  and  $\tau_i = \tau_{i0}$ . We introduce a (small) deformation

$$\begin{aligned}\Delta\kappa_i &= \kappa_i - \kappa_{i0} \\ \Delta\tau_i &= \tau_i - \tau_{i0}\end{aligned}$$

and we expand the energy around the extremum,

$$\begin{aligned}H(\kappa_i, \tau_i) &= H(\kappa_{i0}, \tau_{i0}) + \sum_k \left\{ \frac{\partial H}{\partial \kappa_k|_0} \Delta\kappa_k + \frac{\partial H}{\partial \tau_k|_0} \Delta\tau_k \right\} \\ &+ \sum_{k,l} \left\{ \frac{1}{2} \frac{\partial^2 H}{\partial \kappa_k \partial \kappa_l|_0} \Delta\kappa_k \Delta\kappa_l + \frac{\partial^2 H}{\partial \kappa_k \partial \tau_l|_0} \Delta\kappa_k \Delta\tau_l + \frac{1}{2} \frac{\partial^2 H}{\partial \tau_k \partial \tau_l|_0} \Delta\tau_k \Delta\tau_l \right\} + \mathcal{O}(\Delta^3)\end{aligned}\quad (64)$$

The first term evaluates the energy at the extremum. Since  $(\kappa_{i0}, \tau_{i0})$  is an extremum each term in the first sum vanishes. To proceed we bring to mind that the energy and thus its expansion (64) only depends on  $\kappa_i$  and  $\tau_i$  in a  $SO(2)$  gauge invariant manner. Accordingly, to the leading nontrivial order the expansion should coincide with the discretized version of the energy function (44): We rename  $(\Delta\kappa, \Delta\tau) \rightarrow (\kappa, \tau)$  that we identify with the geometrically determined bond and torsion angles defined in figure 4. Following the steps from (3) to (5) and up to an overall normalization factor we get

$$H(\kappa, \tau) = \sum_{i=1}^{N-1} (\kappa_{i+1} - \kappa_i)^2 + \sum_{i=1}^N \left\{ \lambda (\kappa_i^2 - m^2)^2 + \frac{d}{2} \kappa_i^2 \tau_i^2 - b \kappa_i^2 \tau_i - a \tau_i + \frac{c}{2} \tau_i^2 \right\} \quad (65)$$

For a detailed discussion of (65) we refer to [9, 10]. Since the arguments that lead to (65) are based entirely on general symmetry principles that are universally valid, the result (65) is *unique* for small fluctuations around a given background: The energy (65) engages the complete set of gauge invariant quantities, in terms of the bond and torsion angles, that emerge at leading order in a systematic Taylor expansion of the full energy around its local extremum.

The derivation of (65) utilizes only universal principles. It describes the structure and dynamics of *any* piecewise linear polygonal string, in the leading order of the fluctuations around the fixed background, as an extremum of the free energy. In particular, in the case of proteins, any energy function that describes the dynamics, either at all-atom level or at coarse-grained level, *must* reproduce (65) in the appropriate small fluctuation limit.

For a complete treatment of Hamiltonian dynamics, the Poisson brackets of the variables  $(\kappa_i, \tau_i)$  need to be determined. The brackets that appear in the integrable DNLS hierarchy [18, 19] can be utilized.

### XIV. DISCRETIZED SOLITONS

The energy (65) is a variant of the energy that yields the discrete nonlinear Schrödinger (DNLS) equation [18, 19, 23]: The first term together with the  $\lambda$  and  $d$  dependent terms

constitute the (naively) discretized Hamiltonian of the NLS model in the Hasimoto variable. The conventional DNLS equation is known to support solitons. Thus we can try and find soliton solutions of (65).

As in (46) we first eliminate the torsion angle,

$$\tau_i[\kappa] = \frac{a + b\kappa_i^2}{c + d\kappa_i^2} = a \frac{1 + \hat{b}\kappa_i^2}{\hat{c} + \hat{d}\kappa_i^2} \equiv a\hat{\tau}_i[\kappa] \quad (66)$$

For bond angles we then have

$$\kappa_{i+1} = 2\kappa_i - \kappa_{i-1} + \frac{dV[\kappa]}{d\kappa_i^2} \kappa_i \quad (i = 1, \dots, N) \quad (67)$$

where we set  $\kappa_0 = \kappa_{N+1} = 0$ , and  $V[\kappa]$  is given by (49). This equation is a deformation of the conventional DNLS equation, it is not integrable *a priori*. For a numerical solution, we convert (67) into the following iterative equation [30, 31]

$$\kappa_i^{(n+1)} = \kappa_i^{(n)} - \epsilon \left\{ \kappa_i^{(n)} V'[\kappa_i^{(n)}] - (\kappa_{i+1}^{(n)} - 2\kappa_i^{(n)} + \kappa_{i-1}^{(n)}) \right\} \quad (68)$$

Here  $\{\kappa_i^{(n)}\}_{i \in N}$  denotes the  $n^{\text{th}}$  iteration of an initial configuration  $\{\kappa_i^{(0)}\}_{i \in N}$  and  $\epsilon$  is some sufficiently small but otherwise arbitrary numerical constant; we often choose  $\epsilon = 0.01$ . The fixed point of (68) is clearly a solution of (67). Once the numerically constructed fixed point is available, we calculate the corresponding torsion angles from (66). Then, we obtain the frames from (58) and proceed to construct the discrete string by (59).

At the moment we do not know of an analytical expression of the soliton solution to the equation (67). But we have found [32–34] that an *excellent* approximative solution can be obtained by discretizing the topological soliton (43).

$$\kappa_i \approx \frac{m_1 \cdot e^{c_1(i-s)} - m_2 \cdot e^{-c_2(i-s)}}{e^{c_1(i-s)} + e^{-c_2(i-s)}} \quad (69)$$

Here  $(c_1, c_2, m_1, m_2, s)$  are parameters. The  $m_1$  and  $m_2$  specify the asymptotic  $\kappa_i$ -values of the soliton. Thus, these parameters are entirely determined by the character of the regular, constant bond and torsion angle structures that are adjacent to the soliton; these parameters are not specific to the soliton *per se*, but to the adjoining regular structures. The parameter  $s$  defines the location of the soliton along the string. This leaves us with only two loop specific parameter, the  $c_1$  and  $c_2$ . These parameters quantify the length of the bond angle profile that describes the soliton.

For the torsion angle, (66) involves one parameter ( $a$ ) that we have factored out as the overall relative scale between the bond angle and torsion angle contributions to the energy. Then, there are three additional parameters ( $b/a, c/a, d/a$ ) in the remainder  $\hat{\tau}[\kappa]$ . Two of these are again determined by the character of the regular structures that are adjacent to the soliton. As such, these parameters are not specific to the soliton. The remaining single parameter specifies the size of the regime where the torsion angle fluctuates.

The profile (69) is translation invariant. But on a lattice translation invariance is commonly broken by the Peierls-Nabarro barrier [35]: When the soliton moves along the backbone lattice, quasi-particle waves are emitted in its wake. These waves drain the kinetic energy of the soliton, and cause it to decelerate. Eventually the soliton becomes pinned to a particular backbone site and is unable to translate.

Once the soliton profile  $(\kappa_i, \tau_i)$  is known, we construct the ensuing discrete space string from (58), (59). In the case of a protein backbone as shown in figures 3, 4 where the vertices  $\mathbf{r}_i$  coincide with the positions of the skeletal C $\alpha$  atoms, we use a fixed value in (59),

$$|\mathbf{r}_{i+1} - \mathbf{r}_i| = 3.8 \text{ \AA}$$

for the distance between neighboring vertices. The only exception is *cis*-proline in which case the distance 2.8 \AA should be used; these are *very* rare. In our computations we shall also impose the steric constraint that prevents backbone self-crossing, in terms of the self-avoidance condition [36]

$$|\mathbf{r}_i - \mathbf{r}_k| > 3.8 \text{ \AA} \quad \text{for } |i - k| \geq 2 \quad (70)$$

On the regions adjacent to a soliton, we have constant values of  $(\kappa_i, \tau_i)$ . In the case of a protein, these are the regions that correspond to the standard regular secondary structures. For example, the standard  $\alpha$ -helix is

$$\alpha - \text{helix} : \quad \begin{cases} \kappa \approx \frac{\pi}{2} \\ \tau \approx 1 \end{cases} \quad (71)$$

and the standard  $\beta$ -strand is

$$\beta - \text{strand} : \quad \begin{cases} \kappa \approx 1 \\ \tau \approx \pi \end{cases} \quad (72)$$

Similarly, all the other familiar regular secondary structures such as 3/10 helices, left-handed helices *etc.* are described by definite constant values of  $\kappa_i$  and  $\tau_i$ . Protein loops are regions which are described by the soliton proper. The solitons interpolate between the regular structures, along a protein loop the values of  $(\kappa_i, \tau_i)$  are variable.

Finally, in the case of a super-secondary structure (65) should be properly interpreted as the internal Landau free energy, above the background of a regular secondary structure with constant values of  $\kappa_i$  and  $\tau_i$ .

## XV. PROTEINS AND THE DIRAC PROBLEM OF LIFE

Proteins are delicate nano-scale machines. Like other high precision machines, the way proteins function can be very sensitive to their conformation. The *protein folding problem* was originally posed some 50 years ago, and it has since then assumed various incarnations [37–39]. The problem endures as one of the most important unresolved problems in science, it aims to explain what is life. The *Sampo* would be a theoretical and computational framework, that predicts the shape and describes the dynamics of a protein in its biological environment. The scale, complexity and trophy of the endeavor are enormous: There are some 25 million protein sequences that have been identified through DNA sequencing. But thus far only around 100.000 structures have been experimentally determined [40]. Apparently, the average cost of a structure determination by x-ray crystallography is around 100 kUSD and crystallization of a protein can sometimes take even years, if at all possible. We can hardly expect that the structures of a much larger percentage of sequences can ever be determined using the presently available experimental techniques. Therefore, the development of an accurate and reliable theoretical and computational approach is pivotal for our ability to understand proteins, to resolve the problem of life.

Moreover, a wrong fold is recognized as a common cause for a protein to lose its function. Misfolded proteins can be dangerous, even fatal, to a biological organism. For example neurodegenerative diseases like Alzheimers and Parkinsons, diabetes-II, and many forms of cancer, are all caused by wrong folds in certain proteins. At the same time, the ability to elicit controlled protein misfolding might enable us to combat viral diseases like HIV and coronaviruses (SARS) where no effective treatment presently exist. Controlled protein misfolding might eventually even open the door for the development of new generation molecular level antibacterials, to offset the emergence of resistance through evolutionary processes that are rapidly rendering many existing antibiotics ineffective.

There are, clearly, very many very good reasons to address the *Third Dirac Problem*.

## XVI. YEARNING FOR THE SPEED OF LIFE

Among the goals of all-atom molecular dynamics (MD) is to provide an *ab-initio* description of protein folding and dynamics. MD utilizes finely tuned force fields like Charmm [41] and Amber [42] that aspire to model all known (semi)classical interactions between all the atoms, both in the protein and in the surrounding solvent (water). The Newtonian equations of motion are introduced, for each and every atom, including solvent. The equations are numerically integrated with a time step around a femtosecond, which is the characteristic time scale of peptide bond vibrations. Using purpose built supercomputers like *Anton* [43, 44] and distributed computing projects like *folding@home* [45], the speediest MD simulations can reach a few micro-seconds of *in vivo* folding time, in a day *in silico* [44]. This enables the modeling of relatively short and very fast folding proteins such as villin headpiece (HP35) and the  $\lambda$ -repressor protein (1LMB in Protein Data Bank PDB [40]), up to time scales that it takes for these proteins to fold.

But most proteins are considerable longer and fold during much longer time scales. For example, myoglobin which is a protein described in all biochemistry textbooks, has 154 residues and folds in about 2.5 seconds [46]. Thus, running at top speed of a few micro-seconds per day it should take *Anton* over 1.000 years to fold a myoglobin [44]. And *Anton* is by far the fastest special-purpose MD machine ever built. Accordingly we need some  $10^{11}$  orders of magnitude more in computer speed before MD simulations of proteins like myoglobin will take place *in silico* at the *speed of life*. Provided there is no compelling need to substantially increase the number of atoms involved. Apparently the development of processors with an ever increasing clock speed has stalled. As a consequence modeling of long time scale protein dynamics using all-atom molecular dynamics at the speed of life does not appear realistic, in the foreseeable future.

Moreover, it does also appear that the presently available computers are incapable of handling sufficiently many individual atoms. As a consequence several essential all-atom ingredients still remain to be tackled by implicit and effective methods *in lieu* of all-atom. An important example is acidity, in case of explicit water. The proper level of acidity is pivotal to numerous biological processes. Sometimes even a slight shift in acidity leads to a major change in protein structure and function. A good example is amylin [53]. It is a short polypeptide hormone that has been implicated in the onset of type-II diabetes. Much remains to be done to understand how amylin functions. In order to comprehensively mimic its properties computationally, one needs to perform simulations that model amylin both inside the  $\beta$ -cell granules of pancreas where  $\text{pH} \approx 5.5$ , and in the extra-cellular domain

with  $\text{pH} \approx 7.4$  and where the disease causing amyloidosis takes place; plus through the cell membrane. The structure of amylin seems to be very different, in the two different pH environs. For an all-atom simulation to tackle the difference, suppose we introduce  $10^9$  explicit water molecules which is 4-5 orders of magnitude more than what is presently possible, even with *Anton*. However, this only gives leeway for a mere few tens of explicit hydronium ions, to model the physiological  $\text{pH} \approx 7.4$  at all-atom level. This is hardly enough: When it comes to acidity, today's all-atom remains far from all atoms.

We dare to propose that, all-in-all, some 15 orders of magnitude increase, or even more, in the speed of computer simulations is needed before a copious and accurate all-atom description of protein folding dynamics at the speed of life becomes a reality. This is an enormous number, apparently comparable to or even exceeding the combined national debt of both USA and the EU countries, in roubles. From this perspective the protein folding problem sounds like doomed to endure among the pre-eminent unresolved conundrums in science, for a long time to come. However, this enormous gap between the speed of life and the available speed *in silico* is also an excellent opportunity: There is a vast *Every Man's Land* available for the development of alternative, computationally effective approaches. For this purpose, various coarse-grained models are being developed. Contributions to the all-atom force fields that are presumed to be less relevant, are systematically eliminated. A simplified geometry can also be used. For example, the UNRES [47] force field provides a very detailed and finely tuned coarse grained potential energy with some 15 different terms, in combination with a simplified geometry. Present coarse-graining can extend all-atom MD simulations by some 4-5 orders of magnitude. This considerable success of coarse-graining raises the question, what are the truly relevant contributions to the free energy function.

We note that there are also highly simplified approaches such as the Gō model [48] and its variants. In a Gō-type model one constructs the energy function from the knowledge of all atomic positions and native contacts in the protein of interest: There are as many, or even more parameters than there are atomic positions. As a consequence these approaches do not have any predictive power for the native fold. But they can still be profited *e.g.* to study how the folding might proceed.

In addition, there are several highly successful non-Physics based approaches to the protein folding problem: Structural classification schemes [49, 50] reveal that despite enormous diversity in the amino acid edifice, the number of different folds observed in PDB structures is quite small. This empirical observation forms the conceptual basis for *de novo* structure prediction methods [51]. The basic idea is to utilize properly chosen fragments that are found in the protein conformations which have already been deposited in the PDB database, as modular building blocks very much like *Lego bricks* to construct a folded protein. These comparative methods have the best predictive power [52] for crystallographic folded protein structure, at the moment. However, the lack of a well grounded energy function impedes their utility in investigations of dynamical aspects like the way how the folding takes place.

Finally, what to some might appear as a sign of desperation, we mention and recommend the on-line gaming experience *Foldit*

<http://fold.it>

The players help scientists to discover and determine how a given protein might fold. Best players display an impressive ability to do so, they sometimes even beat scientific approaches.

## XVII. THERMOSTATS

Among the theoretical issues where we trust important progress remains to be made, is the development of thermostats [54]. Molecular dynamics integrates the all-atom Newton's equations of motion, hence the total energy is a conserved quantity. As a consequence MD describes a protein in a microcanonical ensemble. But this does not correspond to *in vivo*: The biological environ of a protein is characterized by a constant temperature, the natural habitat of life in balance is in a canonical ensemble. A native state of a protein which is in (local) thermodynamical equilibrium with its environ corresponds to a local minimum of the Helmholtz free energy

$$H = E - TS \quad (73)$$

where  $E$  is the appropriate internal energy,  $T$  is temperature and  $S$  is the entropy; we overlook volume effect. Note that the entropic forces that derive from  $S$  are pivotal for a protein collapse. In order to describe this *in vivo* environment, the all-atom Hamiltonian Newton's equations need to be modified to mimic a constant temperature setting. For this purpose diverse thermostats have been developed. They facilitate the MD simulation of protein folding, mostly under stationary non-equilibrium conditions. It remains a delicate challenge to construct a purely Hamiltonian thermostat that both models the canonical ensemble of the original system, and allows for a computationally effective discretization for speedy reliable simulations.

Thermostatting often involves a deformation of the all-atom Newton's equation into a Langevin equation. However, such an equation is both non-deterministic and lacks time-irreversibility, and the original impetus to consider a Hamiltonian framework becomes lost. Unfortunately, it appears impossible to construct a canonical thermostat Hamiltonian that has both a finite number of thermostat variables and a non-singular potential. Maybe the most widely used canonical thermostat in MD simulations of protein folding is the one by Nosé and Hoover [55, 56]. In its simplest variant the thermostat has a Hamiltonian character, albeit with a singularity. The all-atom phase space is extended by a single *ghost* particle with a logarithmically divergent potential, its rôle is to provide temperature for all the rest.

We consider a thermostatted extension of (42)

$$S = \int_{-\infty}^{\infty} dt \left\{ \frac{1}{2} q^2 \kappa_t^2 + V[\kappa] + \frac{1}{2} q_t^2 + T \ln q \right\} \quad (74)$$

We assume that  $V[\kappa]$  has a double-well profile. When  $q(t) \equiv 1$  we interpret  $S$  as the Euclidean action of  $\kappa$ ; The variable  $q$  is akin the Nosé-Hoover thermostat, with  $\kappa$  a single generic coordinate of the thermostatted system.

A finite value of (74) is imperative so that the semi-classical amplitude of the coordinate  $\kappa$  to cross over the potential barrier between the two distinct minima of  $V[\kappa]$ , is finite. We are interested in the effect of the thermostat  $q$  on the barrier crossing amplitude. The equations of motion are

$$q^2 \kappa_{tt} = V_{\kappa} - 2q q_t \kappa_t \simeq V_{\kappa} - \gamma \kappa_t \quad (75)$$

$$q q_{tt} = q^2 \kappa_t^2 + T \quad (76)$$

Note that the coupling between  $\kappa$  and the thermostat variable gives rise to an effective friction-like coefficient  $\gamma(t)$ . In the absence of  $q$ , we assume the equation (75) supports a

finite action instanton, *e.g.* with a profile that resembles (43). We inquire whether (74) continues to support a finite action instanton, in the presence of the thermostat.

Suppose

$$\kappa(t) \xrightarrow{t \rightarrow \pm\infty} \kappa_{\pm}$$

where  $\kappa_{\pm}$  are values of the coordinate  $\kappa$  at the opposite sides of the potential barrier. Then, for finite action we obtain the Gibbsian format

$$q(t) \xrightarrow{t \rightarrow \pm\infty} q_{\pm} = e^{-\frac{1}{T}V[\kappa_{\pm}]} \quad (77)$$

This proposes that  $T$  is like temperature, when positive valued. We integrate (76),

$$\int_{-\infty}^{\infty} dt \{q_t^2 + q^2 \kappa_t^2\} = - \int_{-\infty}^{\infty} dt T$$

For a finite Euclidean action (74), the integral on the *l.h.s.* is finite. Since it is non-negative, the temperature  $T$ , if indeed positive, must vanish. For finite  $S$ , we deduce that  $q(t)$  can not be viewed as a variable that yields an equation of motion, it is merely a fixed background field with a fixed profile and no dynamics: For an instanton to persist any dynamical thermostat field  $q(t)$  should become *entirely* decoupled.

We conclude that thermostating should be performed with due care. Impetuous thermostating can disfigure the non-perturbative structure. Even to the extent that soliton-like configurations entirely disappear. This would be unfortunate: We proceed to argue that topological solitons are the modular building blocks of folded proteins.

## XVIII. SOLITONS AND PROTEINS

Various taxonomy schemes such as CATH and SCOP [49, 50] reveal that folded proteins have a modular build. Novel topologies are rare, to the extent that some authors think most modular building blocks are already known [57, 58]. This convergence in protein architecture is a palpable manifestation that protein folding is driven by a universal structural self-organization principle.

We argue that a DNLS soliton is the *auriga praecipua*. Indeed, it has been shown that over 92% of all  $C\alpha$ -traces of PDB proteins can be described by 200 different parametrizations of the discretized NLS kink (69), with better than 0.5 Å root-mean-square-distance (RMSD) precision [34]. Accordingly, we set up to describe the modular building blocks of proteins in terms of various parametrizations of the DNLS soliton profile, that is described by the equations (68), (66), (58) and (59).

From the  $C\alpha$  coordinates of a given protein, available at PDB, we compute the backbone bond and torsion angles. For this we *initially* fix the  $\mathbb{Z}_2$  gauge in (63) so that all the bond angles take positive values. A generic profile consists of a set of  $\kappa_i$ , typically between  $\kappa_i \approx 1$  and  $\kappa_i \approx \pi/2$  and the upper bound is due to steric constraints. The torsion angle values  $\tau_i$  are much more unsettled, they jump over the entire range from  $-\pi$  to  $+\pi$ . In figure 5 we show as an example the  $(\kappa_i, \tau_i)$  spectrum in the case of the  $\lambda$ -repressor protein, with PDB code 1LMB. The spectrum is fairly typical, for a PDB configuration.

The  $C\alpha$  backbone of a protein is piecewise linear, the spectrum of  $(\kappa_i, \tau_i)$  is discrete. The general bifurcation analysis in Sections X and XI relates to a continuous string, with



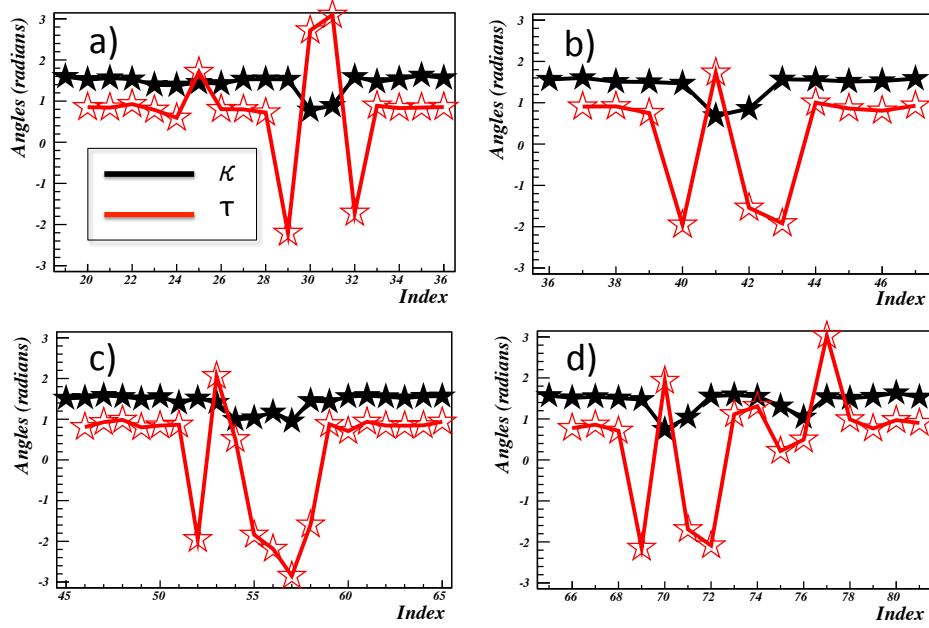


FIG. 5: The bond angle ( $\kappa$ ) and torsion angle ( $\tau$ ) spectrum of  $\lambda$ -repressor 1LMB; the indexing follows PDB.

differentiable curvature and torsion. Thus we need an extension of the general results to the specific case of a piecewise linear string: We continue to interpret a change in the sign of  $\tau_i$  in terms of a flattening point. It suggests that an inflection point perestroika has taken place. Accordingly, we implement a series of  $\mathbb{Z}_2$  gauge transformations (63) in the vicinity of putative flattening points where  $\tau_i$  changes sign or is otherwise unsettled, to identify the putative multi-soliton profile in  $\kappa_i$ . For example, in the case of 1LMB there are four regions with an irregular  $\tau_i$  profile. By a judicious choice of  $\mathbb{Z}_2$  gauge transformations we identify seven different solitons (69) in  $\kappa_i$ . The profiles are shown in figure 6. Each of the soliton profile is clearly accompanied by putative flattening points; note the multivaluedness of  $\tau_i$ . The general considerations in Sections X and XI, albeit developed for the case of continuous strings, are very much in line with the analysis of a generic discrete C $\alpha$  protein profile. We conclude that protein folding is due to inflection and flattening point perestroika's. These bifurcations deform the C $\alpha$  backbone and create DNLS solitons along it.

In the case of our example 1LMB, the seven  $\mathbb{Z}_2$  gauge transformed soliton profiles define the background, around which we perform the expansion (64), (65). For this we first train the energy function to describe the background. In practice we do the training by demanding that the fixed point of the iterative equation (68) models the C $\alpha$  backbone as a DNLS multi-soliton solution, and with a prescribed precision. We have developed a program *GaugeIT* that implements the  $\mathbb{Z}_2$  gauge transformations to identify the background, and we have developed a program *PropoUI* to train the energy so that its extremum models the background as a multi-soliton. The programs are described at

$$\text{http} : // \text{www.folding} - \text{protein.org} \quad (78)$$

In the case of a protein for which the PDB structure is determined with an ultra-high resolution, typically below 1.0 Ångström, *PropoUI* routinely constructs a multi-soliton that

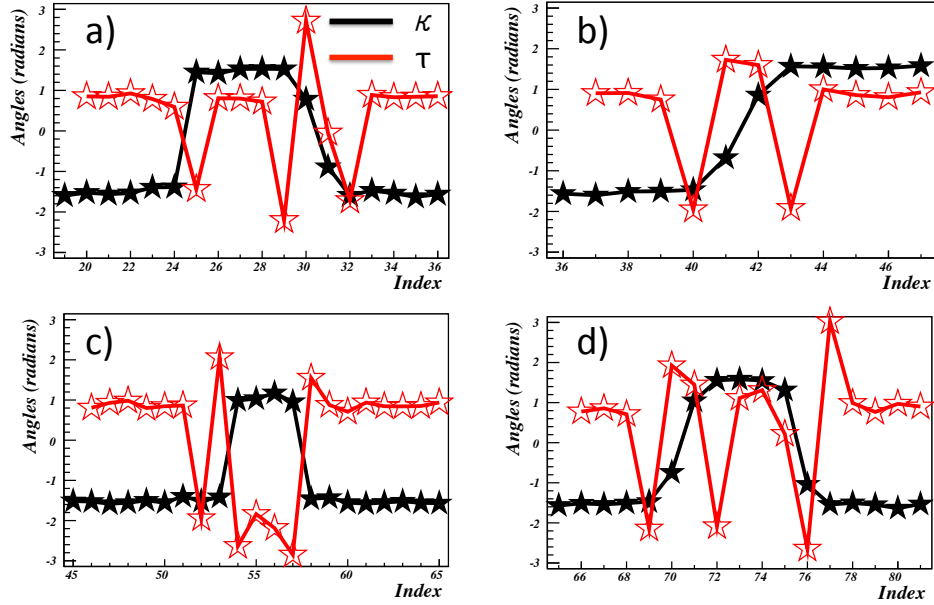


FIG. 6: The  $\mathbb{Z}_2$  gauge transformations of the bond angle ( $\kappa$ ) and torsion angle ( $\tau$ ) spectrum of  $\lambda$ -repressor 1LMB; the indexing follows PDB.

describes the  $C\alpha$  backbone with the experimental precision: The accuracy of a given experimental PDB structure can be estimated from the B-factors using the Debye-Waller formula. It relates the experimental B-factor to the one standard deviation fluctuation distance in the  $C\alpha$  position

$$\sqrt{\langle \mathbf{x}^2 \rangle} \approx \sqrt{\frac{B}{8\pi^2}} \quad (79)$$

The B-factors are available in PDB. In figure 7 we compare the distance between the  $C\alpha$  backbone, the DNLS soliton solution, and the B-factor fluctuation distance in the experimental structure 1LMB. As shown in the figure, the DNLS soliton describes the backbone with a precision that is fully comparable with the experimental uncertainties. The grey zone around the soliton profile denotes our best estimate for the extent of quantum mechanical zero-point fluctuations. By analyzing available crystallographic PDB structures we have concluded that the quantum mechanical fluctuations in the positions of the  $C\alpha$  atoms should not exceed 15 pico meters. This estimate coincides with the historically used value, for the wavelength boundary between x-rays and  $\gamma$ -rays.

Simulations that have been performed using the UNRES force field, thus far, support that folded proteins display a soliton driven structural self-organization. Furthermore, the cause of protein folding can be traced to a combination of inflection point and bi-flattening perestroika's. At least in the case of protein-A [59].

## XIX. FOLDING AT THE SPEED OF LIFE

By construction, the expression (65) of the energy is *universal*: It is the leading infrared contribution to the expansion (64) of the full Helmholtz free energy (73), around a generic

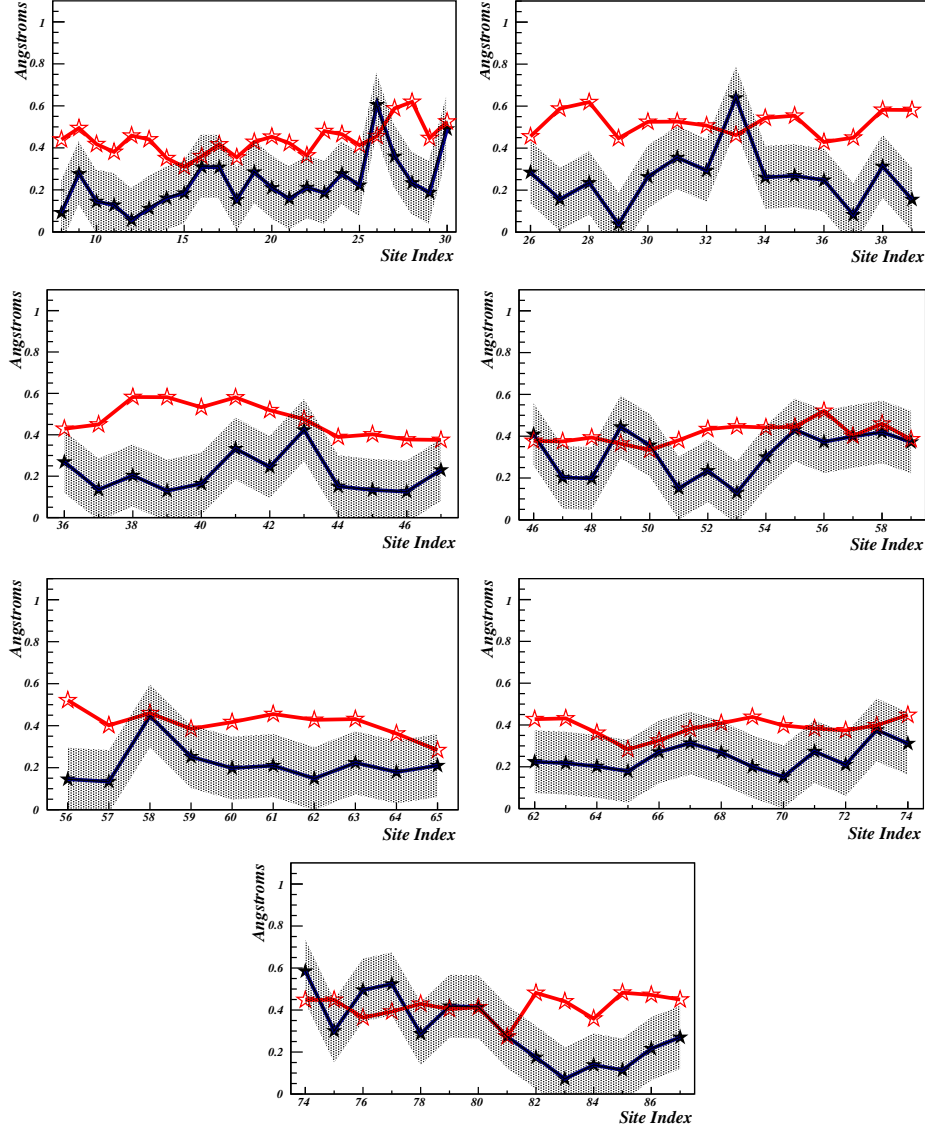


FIG. 7: The distance between the PDB backbone of the first 1LMB chain and its approximation by the seven solitons solutions. The black line denotes the distance between the soliton and the corresponding PDB configuration. The grey area around the black line describes our estimate of 15 pico meter (essentially quantum mechanical) zero point fluctuation distance around each soliton. The grey (red) line denotes the Debye-Waller fluctuation distance (79).

but pre-determined extremum. Thus (65) describes the energy landscape of a protein, not only at the extremum but also in its vicinity. The expansion (65) can be utilized to explore the near-equilibrium dynamics, such as the way how the protein responds to temperature fluctuations and variations in other environmental parameters, acidity and so forth.

In particular, the present approach is designed to facilitate the description of protein dynamics over biologically relevant time scales. It averages over all very short time scale atomic level oscillations, vibrations, and those tiny fluctuations and deformations in the positions of the individual atoms that are more or less irrelevant to the way how the folding

progresses over time scales that are biologically important.

To describe non-equilibrium dynamics, we adopt a Markovian Monte Carlo (MC) time evolution with the universal heat bath probability distribution (Glauber dynamics) [60, 61]

$$\mathcal{P} = \frac{x}{1+x} \quad \text{with} \quad x = \exp\left\{-\frac{\Delta E}{kT}\right\} \quad (80)$$

Here  $\Delta E$  is the energy difference between consecutive MC time steps, that we compute from (65). It can be proven [62, 63] that MC simulation with (80) approaches the Gibbsian distribution at exponential rate. Thus, the method should provide a statistically meaningful description of near-equilibrium protein folding dynamics, at least during adiabatic temperature variations.

In our simulations of near-equilibrium proteins, we renormalize the numerical value of the temperature factor  $kT$  so that it coincides with the experimentally observed  $\theta$ -point temperature [64]. We proceed as follows: We start by training (64), (65) to describe a given, typically very low temperature crystallographic PDB protein configuration as a multi-soliton. For this we utilize the program *Propro* that we have described in (78). Once the multi-soliton has been constructed, we subject it to extensive heating and cooling simulations. We start from a vanishingly low temperature value, with no apparent thermal fluctuations in the C $\alpha$  positions. We slowly increase the temperature until we observe a structural transition akin a phase transition, above which the configuration resembles a random walker. The transition identifies the renormalization point of the temperature factor, it takes place at the  $\theta$ -point temperature. A convenient order parameter for detecting the  $\theta$ -point is the C $\alpha$ -trace radius of gyration [65, 66]

$$R_g^2 = \frac{1}{2N^2} \sum_{i,j} (\mathbf{r}_i - \mathbf{r}_j)^2 \xrightarrow{N \text{ large}} R_0^2 N^{2\nu} \quad (81)$$

Here  $\nu$  is the compactness index that governs the large- $N$  asymptotic form of equation (81), and  $R_0$  is a form factor that characterizes the effective distance between the C $\alpha$  atoms in the large  $N$  limit. The compactness index  $\nu$  is a universal quantity but the form factor  $R_0$  is not. The form factor is in principle a calculable quantity, from the atomic level structure of the protein and the surrounding solvent.

In figure 8 we show, as an example, how the C $\alpha$  root-mean-square-distance (RMSD) between the crystallographic X-ray myoglobin structure with PDB entry code 1ABS and its multi-soliton description constructed using (64), (65) evolves, when we increase and decrease the temperature. In this simulation we first heat up the multi-soliton. We thermalize it in the  $\theta$ -regime. We then cool it down, back to low temperature values where only very small thermal motion persist.

Generically, in the case of proteins with a well defined native state such as myoglobin and  $\lambda$ -repressor, both of which we have already introduced as examples, we recover the initial configuration with a very high RMSD precision as shown in figure 8. But for a protein that is intrinsically disordered, an example is amylin that we described in Section XVI, this is not the case. For an intrinsically disordered protein we commonly find a complex conformational landscape in the low temperature limit.

In the case of myoglobin, when we start from a random configuration above the  $\theta$ -point temperature, say 380K in figure 8, we reach the native state in over 99 per cent of cooling simulations within 3.5 seconds using a single processor in MacBook Air. This can be contrasted to the experimentally measured *in vivo* folding time which is 2.5 seconds [46]. Thus,

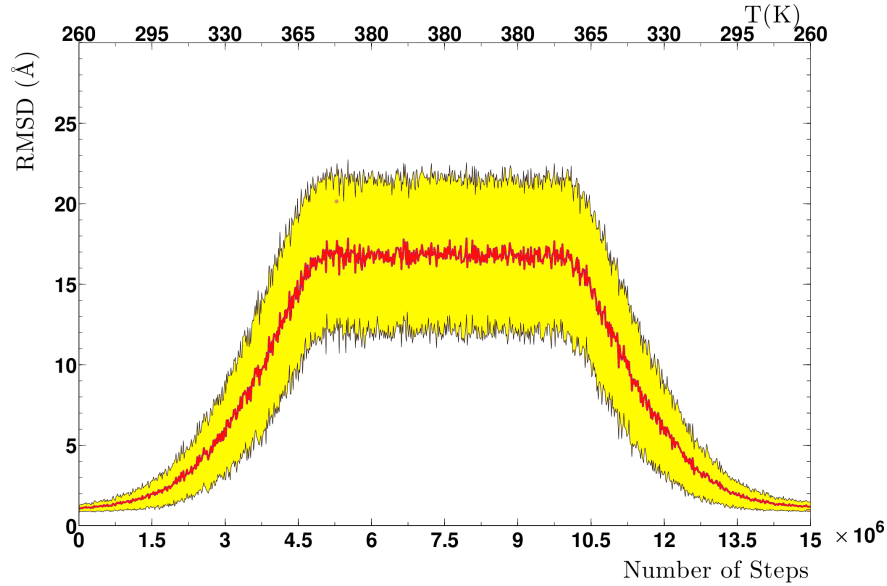


FIG. 8: The evolution of the root-mean-square distance (RMSD) between the myoglobin PDB entry 1ABS backbone, and the simulated multi-soliton configuration. The (red) line is the average of 1.000 simulations, and the surrounding (yellow) shaded area describes the one standard deviation extent of fluctuations. Along the top axis, we have converted the temperature into Kelvin scale, using the renormalization procedure described in [67].

by describing proteins as multi-solitons it is quite possible to reach the *speed of life* with a presently available, standard laptop. Even to exceed it, with a good work-station.

## XX. CONCLUDING REMARK

The collapse of a protein is a complex physical phenomenon that engages a multitude of disparate temporal and spatial scales. In particular, there are many high energy barriers that the protein must be able to overcome as it progresses from a random string towards the native fold. This obligates thousands of atoms to cooperate over quite long time periods, so that complex collective multi-molecule motions can take place and enable the conformation to cross the various steep hurdles and hindrances. These obstacles that come with varying scales and diverse structures, pose major computational bottle-necks in any all-atom approach to the protein folding problem. Thus, a detailed MD simulation of the entire folding process remains a formidable task. But in a seemingly paradoxical manner [68] proteins succeed to fold in the congestion of our cells, very reliably and at a quite high speed.

Similar kind of apparent paradoxes are encountered all over the physical world: Think of water, how quickly it finds a way to self-organize into a wave. Or a typhoon, that commonly emerges in the atmosphere. Each involve the collective cooperation of an enormous number of atomic level constituents, far more than in a protein. Any attempt to an all-atom description would be preposterous. But in each case like in numerous others, we have an exceedingly solid theoretical framework: Korteweg-de Vries equation with its solitons in the former and the vortices of Navier-Stokes equation in the latter. Why not try and use a

similar kind of approach to structural self-organization, also in the case of proteins?

## XXI. ACKNOWLEDGEMENTS:

I am indebted to Ludvig Faddeev for our continuing friendship and scientific collaboration that spans over 25 years. Most of the results presented in this article are based at least indirectly on our joint work, all I do is describe what I have learned by working with him. Ludvig also knows the art of a rich life, and how to enjoy it at full speed. Sometimes, only a feather on the brake (see acknowledgement of reference 15). I wish to thank S.Chen, M.Chernodub, U. Danielsson, M.-L. Ge, J. He, K. Hinsén, Y. Hou, S. Hu, N. Ilieva, T. Ioannidou, Y. Jiang, D. Jin, G. Kneller, A.Krokhotin, J.Liu, A. Liwo, M.Lundgren, G. Maisuradze, N.Molkenthin, X. Nguyen, S. Nicolis, X. Peng, H. Scheraga, F. Sha, A. Sieradzan, A. Sinelkova, M. Ulybyshev and many many others for numerous discussions on various aspects of the research described here. I acknowledge support from Region Centre Recherche d'Initiative Academique grant, Sino-French Cai Yuanpei Exchange Program (Partenariat Hubert Curien), Vetenskapsrådet, Carl Trygger's Stiftelse för vetenskaplig forskning, and Qian Ren Grant at BIT.

- 
- [1] J.E. Cohen, PLoS Biol **2** e439 (2004)
  - [2] P.A.M. Dirac, Proc. Roy. Soc. **A133** 60 (1931)
  - [3] L.D. Faddeev, A.A. Slavnov, *Gauge Fields: An Introduction To Quantum Theory* (Benjamin/Cummings Publishing Company, Inc. Reading, MA 1991)
  - [4] L.P. Kadanoff, Physics **2** 263 (1966).
  - [5] K.G. Wilson, Phys. Rev. **B4** 3174 (1971).
  - [6] M.N. Chernodub, L.D. Faddeev, A.J. Niemi, JHEP **12** 014 (2008)
  - [7] F. Frenet, J. de Math. **17** 437 (1852)
  - [8] A.J. Niemi, Phys. Rev. **D67** 106004 (2003)
  - [9] S. Hu, Y. Jiang, A.J. Niemi, Phys. Rev. **D87** 105011 (2013)
  - [10] T. Ioannidou, Y. Jiang, A.J. Niemi arXiv preprint [arXiv:1403.4401](https://arxiv.org/abs/1403.4401) (Physical Review D, to appear)
  - [11] R.L. Bishop, Am. Math. Mon. **82** 246 (1974)
  - [12] A.J. Hanson, *Visualizing Quaternions*, (Morgan Kaufmann Elsevier, London, 2006)
  - [13] L. Faddeev, A.J. Niemi, Phys. Rev. Lett. **82** 1624 (1998)
  - [14] L. Faddeev, A.J. Niemi, Phys. Lett. **B449** 214 (1999)
  - [15] L. Faddeev, A.J. Niemi, Phys. Lett. **B464** 90 (1999)
  - [16] L. Faddeev, A.J. Niemi, Nucl. Phys. **B776** 38 (2007)
  - [17] H. Hasimoto, J. Fluid. Mech. **11** 477 (1972)
  - [18] L.D. Faddeev and L.A. Takhtajan, *Hamiltonian methods in the theory of solitons* (Springer Verlag, Berlin, 1987)
  - [19] M.J. Ablowitz, B. Prinari and A.D. Trubatch, *Discrete and Continuous Nonlinear Schrödinger Systems* (London Mat. Soc. Lect. Note Series **302**, London, 2003)
  - [20] A.M. Polyakov, Nucl. Phys. **B268** 406 (1986)
  - [21] O. Kratky and G. Porod, Rec. Trav. Chim. **68** 1106 (1949)

- [22] N. Manton and P. Sutcliffe, *Topological Solitons* (Cambridge University Press, Cambridge, 2004)
- [23] P.G. Kevrekidis, *The Discrete Nonlinear Schrödinger Equation: Mathematical Analysis, Numerical Computations and Physical Perspectives* (Springer-Verlag, Berlin, 2009)
- [24] S. Hu, M. Lundgren, A.J. Niemi, Phys. Rev. **E83** 061908 (2011)
- [25] V.I. Arnold, *Singularities of Caustics and Wave Fronts* (Kluwer Academic Publishers, Dordrecht, 1990)
- [26] V.I. Arnold, Russ. Math. Surv. **50** 1 (1995)
- [27] V.I. Arnold, Amer. Math. Soc. Transl. **171** 11 (1996)
- [28] F. Aicardi, Funct. Anal. Appl. **34** 79 (2000)
- [29] R. Uribe-Vargas, Enseign. Math. **50** 69 (2004)
- [30] N. Molkenthin, S. Hu, A.J. Niemi, Phys. Rev. Lett. **106** 078102 (2011)
- [31] M. Herrmann, Applic. Anal. **89** 1591 (2010)
- [32] M. Chernodub, S. Hu, A.J. Niemi, Phys. Rev. **E82** 011916 (2010)
- [33] S. Hu, A. Krokhotin, A.J. Niemi, X. Peng, Phys. Rev. **E83** 041907 (2011)
- [34] A. Krokhotin, A.J. Niemi, X. Peng, Phys. Rev. **E85** 031906 (2012)
- [35] A. Sieradzhan, A.J. Niemi, preprint Uppsala (to appear)
- [36] U.H. Danielsson, M. Lundgren, A.J. Niemi, Phys. Rev. **E82** 021910 (2010)
- [37] K.A. Dill, S.B. Ozkan, M.S. Shell, T.R. Weikl, Annu. Rev. Biophys. **37** 289 (2008)
- [38] K.A. Dill, J.L. MacCallum, Science **338** 1042 (2012)
- [39] B.M. Pettitt, Journ. Biomol. Struct. Dyn. **31** 1024 (2013)
- [40] H.M. Berman, J. Westbrook, Z. Feng, G. Gilliland, T.N. Bhat, H. Weissig, I.N. Shindyalov, P.E. Bourne, Nucl. Acids Res. **28** 235 (2000); <http://www.pdb.org>
- [41] B. R. Brooks, R. E. Bruccoleri, B. D. Olafson, D. J. States, S. Swaminathan, M. Karplus, J. Comp. Chem. **4** 187 (1983)
- [42] J.W. Ponder, D.W. Case, Adv. Protein Chem. **66** 27 (2003)
- [43] K. Lindorf-Larsen, S. Piana, R. Dror, D. Shaw, Science **334** 517 (2011)
- [44] D.P. Scarpazza, D.J. Ierardi, A.K. Lerer, K.M. Mackenzie, A.C. Pan, J.A. Bank, E. Chow, R.O. Dror, J.P. Grossman, D. Killebrew, M.A. Moraes, C. Predescu, J.K. Salmon, D.E. Shaw, 2013 IEEE 27th International Symposium on Parallel and Distributed Processing 933 (2013)
- [45] V.S. Pande, *et.al.* Biopolymers **68** 91 (2003)
- [46] P.A. Jennings, P.E. Wright, Science **262** 892 (1993)
- [47] A. Liwo, Y. He, H.A. Scheraga, Phys. Chem. Chem. Phys. **13** 16890 (2011)
- [48] N. Gō, Ann. Rev. Biophys. Bioeng. **12** 183 (1983)
- [49] T.E. Lewis, S. Addou, A. Cuff, T. Dallman, M. Dibley, O. Redfern, F. Pearl, R. Nambudiry, A. Reid, I. Sillitoe, C. Yeats, J.M. Thornton, C.A. Orengo, Nucl. Acids Res. **35** D291(2007)
- [50] A.G. Murzin, S.E. Brenner, T. Hubbard, C. Chothia, J. Mol. Biol. **247** 536 (1995)
- [51] G.A. Houry, J. Smadbeck, C.A. Kieslich, C.A. Floudas, Trends in Biotech. **32** 99 (2014)
- [52] <http://www.predictioncenter.org/index.cgi>
- [53] P. Westermarck, C. Wernstedt, E. Wilander, D.W. Hayden, T.D. O'Brien, K.H. Johnson, Proc. Natl. Acad. Sci. USA **84** 3881 (1987)
- [54] P.H. Hünenberger, Adv. Polym. Sci. **173** 105 (2005)
- [55] S. Nosé, J. Chem. Phys. **81** 511 (1984)
- [56] W.G. Hoover, Phys. Rev. **A31** 1695 (1985)
- [57] S. Rackovsky, Proteins Struct. Funct. Genet. **7** 378 (1990)
- [58] J. Skolnick, A.K. Arakaki, Y.L. Seung, M. Brylinski, Proc. Natl. Acad. Sci. U.S.A. **106** 15690

- (2009)
- [59] A. Krokhotin, A. Liwo, G. Maisuradze, A.J. Niemi, H.A. Scheraga, *Journ. Chem. Phys.* **140** 025101 (2014)
  - [60] R.J. Glauber, *Journ. Math. Phys.* **4** 294 (1963)
  - [61] A.B. Bortz, M.H. Kalos, J.L. Lebowitz, *Journ. Comput. Phys.* **17** 10 (1975)
  - [62] F. Martinelli, E. Olivieri, *Comm. Math. Phys.* **161** 447 (1994)
  - [63] F. Martinelli, E. Olivieri, *Comm. Math. Phys.* **161** 487 (1994)
  - [64] A. Krokhotin, M. Lundgren, A.J. Niemi, X. Peng, *Journ. Phys. Cond. Mat.* **25** 325103 (2013)
  - [65] P.G. De Gennes, *Scaling Concepts in Polymer Physics* (Cornell University Press, Ithaca, 1979)
  - [66] L. Schäfer, *Excluded Volume Effects in Polymer Solutions, as Explained by the Renormalization Group* (Springer Verlag, Berlin, 1999)
  - [67] A. Krokhotin, A.J. Niemi, X. Peng, *J. Chem. Phys.* **138** 175101 (2013)
  - [68] C. Levinthal, in *Mössbauer Spectroscopy in Biological Systems: Proceedings of a meeting held at Allerton House, Monticello, Illinois* 22 (1969)